



# AMAZALERT Delivery Report

Title	<b>Report on the likely response of the Amazon basin hydrology and river discharge to land use and climate change</b>
Work Package Number	2
Delivery number	2.4
First author	Celso von Randow (INPE)
Co-authors	Hester Biermans Matthieu Guimberteau Fanny Langerwisch Lucas Garofolo Lopes German Poveda Anja Rammig Rita de Cassia S. von Randow Daniel Andres Rodriguez Guilherme Samproгна Mohor José Lázaro Siqueira Junior Kirsten Thonicke Javier Tomasella Hans Verbeeck
Date of completion	
Name leading Work Package Leader	Hans Verbeeck
Approved by the Leading Work Package Leader	YES / NO

## To complete by the Coordinator

Approved by the Coordinator	YES / NO
Date of approval by the Coordinator	

## Table of Contents

Summary .....	3
1. Introduction.....	3
2. Datasets used as input to DGVMs and sub-basin hydrology models .....	4
3. Impacts of Climate and Land Cover change on Evapotranspiration patterns.....	6
4. Possible effects of climate and land use change on river discharge and functionality of hydropower plants.....	10
4.1. Impacts on sub-basin scales .....	11
4.1.1. Sites and Methods Description .....	11
4.1.2. Results.....	17
4.1.3. Conclusions.....	27
4.2. Basin-wide Impacts.....	28
4.2.1. Effects of climate change and land use change on discharge .....	28
4.2.2. Effects of changes in discharge on hydropower generation .....	29
4.2.3. Effects of hydropower generation on downstream ecosystems .....	30
4.2.4. Discussion and conclusion .....	31
5. Effect of climate and land use change on average and extreme flows in the Amazon River basin - A scaling approach .....	32
5.1. Data.....	32
5.2. Water Balance Assessment – Present (1970-2008) .....	33
5.3. Statistical Scaling and Water Balance - Present (1970-2008) .....	34
5.4. Maximum River Flows - Present (1970-2008) vs. Future (2009- 2050).....	36
5.5. Conclusions.....	37
6. References.....	38

## Summary

This document consists of an overview of different research activities performed in AMAZALERT Work Package 2 related to analyses of possible impacts of climate change and land use / land cover change (LUCC) on components of the hydrologic cycle of Amazonia (evapotranspiration and river discharges) and possible implications on the provision of ecosystem services such as water yield for hydropower generation.

Four different land surface models and a distributed hydrological model were run following a standard protocol, forced by scenarios of climate change and three different land use scenarios projected by a land use model: a sustainable, environmental development scenario and two levels of intensive deforestation scenarios, one with a mid-level land demand and one with a strong land demand that emulates strong biofuel targets.

Results obtained in these analyses reflect the collaborative aspect of the project. Partner CNRS with collaborations from UGENT, PIK and INPE analysed the relationship between climate, land-use patterns and evapotranspiration patterns. Partner INPE focused on the smaller scale, using its distributed hydrological model MHD-INPE, and studied impacts on hydropower plants at three sub-basins (tributaries of the Amazon). Partners PIK and ALTERRA also collaborated on analyses of hydropower dams but at the Amazon basin scale. Additionally, Partner UNAL with collaborations from INPE, UGENT, CNRS and PIK analyse average and extreme flows, using basin-wide runoff–climate statistical relationships with outputs from the hydrological model outputs and observations.

## 1. Introduction

The consequences of climate and land-use change for the Amazon regions' water resources are of the most palpable for the regional society. Extremes, low river levels such as in the extremely dry years of 2005 and 2010 (Marengo et al. 2011) are of direct effect to local livelihoods.

It is likely that various policies and development plans for the Amazon region are highly sensitive to disturbances of water resources, and conversely, large-scale hydrology plans such as dams and waterways are likely to affect the river discharge itself. The standard wisdom in landscape hydrology is that deforestation leads to lower evapotranspiration (as surfaces are smoother) and increased runoff, i.e. to increase river discharge. If this were the case for the Amazon, deforestation should lead to increased flooding, more extreme low discharges, and in general should reduce the downwind moisture transport, and recycling in the basin. Compilation of data over the last decades, however, and small-scale catchment studies, seem to show that this effect is absent (Rodriguez et al 2010). Explanations are not clear, but could be related to enhanced energy redistribution, or mesoscale circulation enhancement, between fragmented forests. During AMAZALERT, a detailed study of the impacts of climate and land-use change on the hydrological cycle and functionality of hydropower plants in the Amazon was performed. A standardized model intercomparison protocol was used, with uniform forcing data and land use / land cover projections that served as inputs to drive 4 different large scale land surface models with dynamic vegetation, of which 2 were also explicitly simulating river discharges and one additional detailed hydrological model calibrated to key sub-basins in the Amazon region.

The underlying scientific question is: to what extent do deforestation and spatial patterns thereof, and dams, may affect rainfall-runoff ratios and how does climate change modify this through changed rainfall and evaporative demand?

These questions were then addressed at two scales:

- 1) At the amazon-wide scale, using large-scale river routing schemes in ORCHIDEE and LPJml models, as well as a statistical scaling approach (HydroSIG, Poveda et al, 2007).
- 2) At the scale of three major South Amazon tributaries: the Madeira/Mamore, the Tapajos and the Tocantins river basins. These catchments are selected as test study cases that are both located in dynamic frontiers since include savanna-rainforest transitions and are both part of Brazilian agriculture frontier, under strong pressure for land expansion, and have important hydropower plants currently installed and with plans for new developments.

## 2. Datasets used as input to DGVMs and sub-basin hydrology models

As planned in the AMAZALERT, models have performed 12 “future runs” using 3 different climate forcings and 4 distinct future LUC scenarios. In this section we present a short summary of both the climate forcings as the future LUC scenarios used. All datasets of the climate forcings and future LUC scenarios were distributed to the modelling groups via the Amazalart-UGent webpage.

### *Climate Forcings:*

We used 3 distinct future meteorological climate forcings resulting from the 21<sup>st</sup> century General Circulation models (GCM) projections under IPCC AR4 SRES A2 emission scenario. More specific we examined the bias corrected NCAR-PCM (*Parallel Climate Model*), the bias corrected CCSM (*Community Climate System Model*) and the HadCM3 (*Hadley Centre Coupled Model, version 3*) climate forcings.

Additionally, a set of global climate models was used as input for the hydrological model MHD-INPE: MIROC-5 (Watanabe, 2010); CSIRO-Mk3.6.0 (Rotstayn et al., 2010); IPSL-CM5A-LR (Dufresne et al., 2013); and HadGEM2-ES (Collins et al., 2008), a dynamically downscaled model runs from the Atmospheric Model Eta-INPE over South America (Chou et al., 2011).

### *Future Land Use/Land Cover Scenarios:*

The generation of land cover maps based on these scenarios was performed as Task 2.2, using the LuccME generic modeling framework, developed at INPE. Detailed description of the scenario development and quantification of land use change based on the different scenarios is presented in deliverable 4.2.

Figure 1 synthesizes key elements of the land use dynamics which are represented in the quantification of land use/land cover change in AMAZALERT.

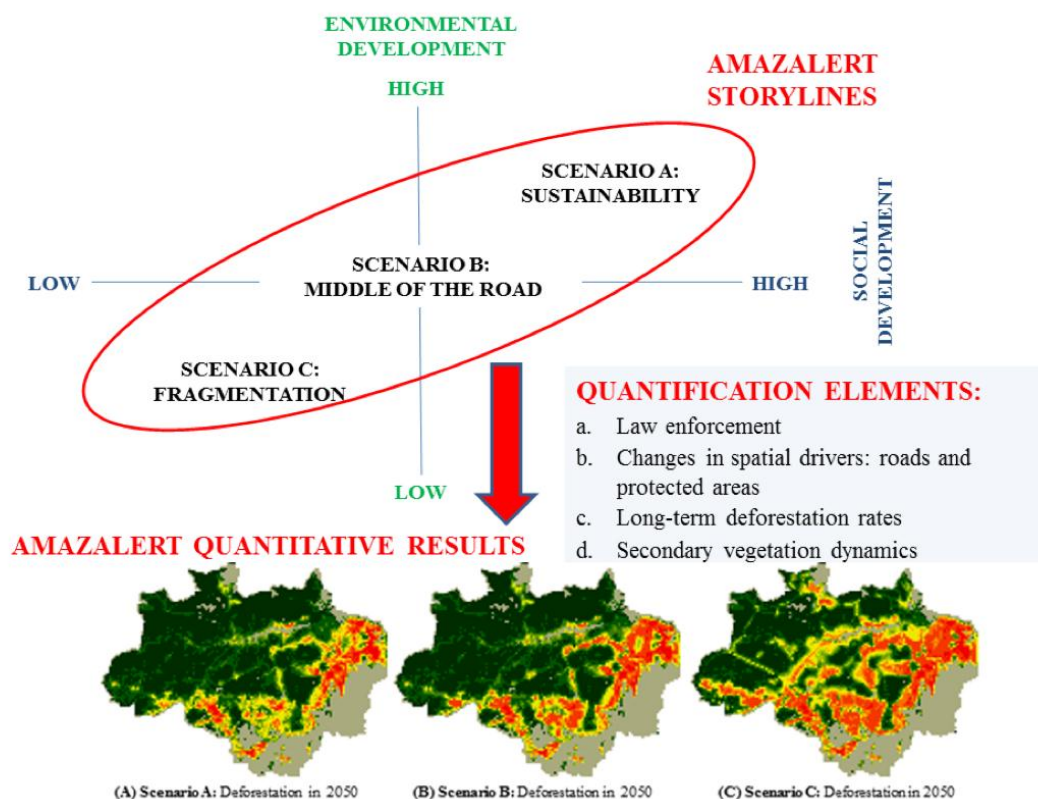


**Figure 1.** Key selected elements used to quantify AMAZALERT land use scenarios in the LuccME framework.

For the analyses of impacts of land use change on hydrology components and effects on hydropower generation, we focused on the two contrasting scenarios of land use, Scenario A and Scenario C, but the latter using two levels of deforestation ‘demand’, either to attend a strong demand of land to fulfill future biofuel targets (which we call the extreme scenario ‘C2’) or not (scenario ‘C1’). The ‘middle of the road’ scenario B was not directly forced to the land surface models.

A fourth land cover map was also considered: a ‘potential vegetation’ map, generated by the DGVMs without considering any effect of land use change. Therefore, the list of land cover maps is as follows:

- **SceA:** Scenario A: Sustainable land use.
- **SceC1:** Scenario C1: Extreme deforestation scenario without strong biofuel targets, resulting in on average 15000 km<sup>2</sup> of deforestation.
- **SceC2:** Scenario C2: Extreme deforestation scenario with strong biofuel targets, resulting in on average 19500 km<sup>2</sup> of deforestation.
- **PotVeg:** Potential Vegetation: Natural development of vegetation without land use change (estimated by the Dynamic Vegetation Models)

### 3. Impacts of Climate and Land Cover change on Evapotranspiration patterns

The fate of the Amazon basin hydrology that faces the climate change and significant deforestation is still unknown. Estimation of this uncertainty in modeling the change in hydrology for the end of the XXI century requires a multi-model approach. Here, we used three dynamic vegetation global models (DVGMs) to simulate the water cycle components. Using bias-corrected AR4 Global Climate Models (GCMs) data sets and new large-scale land cover change (LCC) scenarios, we estimated at sub-basin scale (Figure 2) the Amazon water budget disturbances in the future without atmospheric feedbacks, according to different potential deforestation story lines. Between 7% and 35% of total tree area decrease is projected in the Amazon basin (Figure 3). The most extensive deforestation occurs in the southern sub-basins. Thus, we focus the study over two sub-basins: the Madeira (closed at Fazenda Vista Alegre (FVA)) and the Tapajos (closed at Itaituba (ITA)) basins (see Figure 2) where deforestation is expected to reach 50% according to the more severe scenario (SceC2) (Figure 3). We will mainly study the impact of LCC with this scenario.

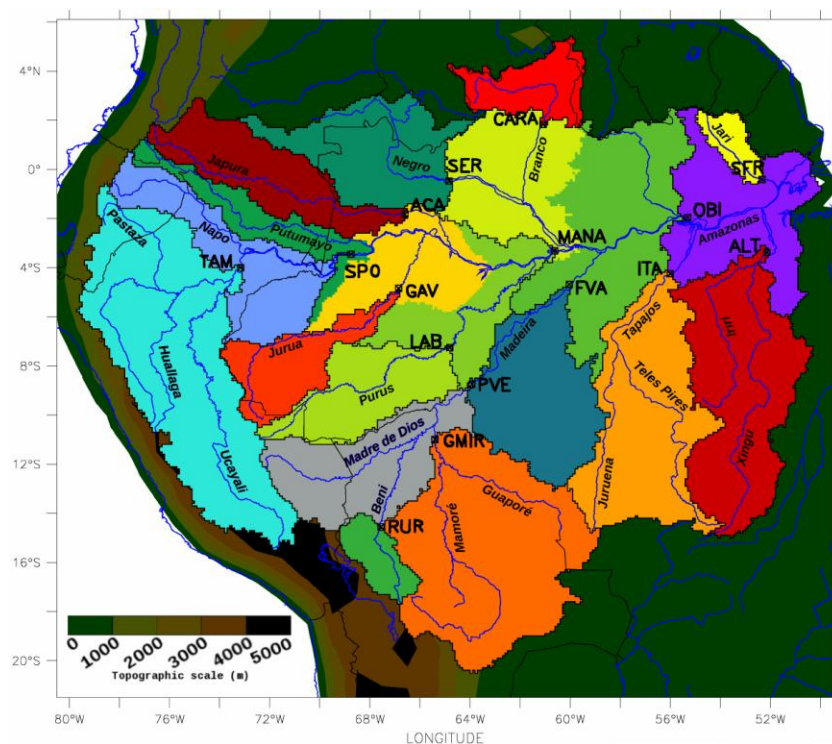


**Figure 2.** Map of the Amazon sub-basins and the main rivers from Guimberteau et al. 2012. Localization of the main ORE HYBAM gauge stations. Color is used to distinguish the different sub-basins. Topographic scale is indicated.

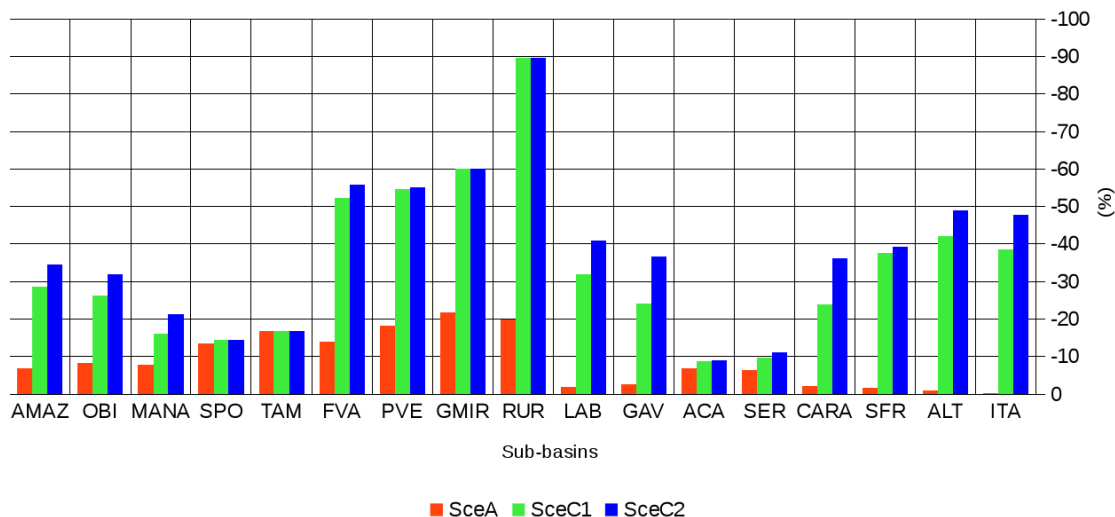


**Figure 3.** Deforestation intensity over the different sub-basins (see Figure X), according to the three land cover scenarios (SceA, SceC1 and SceC2) compared with the scenario without land cover change (PotVeg).

Over the whole Amazon basin, only low decrease in annual ET is simulated by the models due to LCC (between 0.5% to 3%) irrespective of the future forcing, even under the most severe deforestation scenario (SceC2). Yet, in the southern region where a marked dry season occurs during the middle of the year, the impact of LCC on JJA ET is higher. Figure 4 points out the general JJA ET decrease over the Madeira and the Tapajos basins, when the results from the nine simulations (3 forcings x 3 DVGMs) are averaged (up to more than 0.4mm/d of ET decrease in the southern Tapajos, Figure 4). The consensus on simulating ET decrease in the southern Tapajos is affected by the fact that LPJml simulates an ET increase with two future forcings. An ET decrease by 20% is reached with the model ORCHIDEE forced by the HAD forcing (Figure 4).

Over the Madeira basin, highest ET decrease simulated by INLAND and ORCHIDEE occurs during the end of the dry season (up to 0.2mm/d) (Figure 5a). ET variation over the Tapajos basin is more pronounced (Figure 5b) and occurs during the dry season with INLAND and ORCHIDEE (up to -0.6mm/d with ORCHIDEE) and later with LPJml (in October). We notice that the uncertainty of the magnitude in ET decrease due to the future forcing is much larger with ORCHIDEE, mainly in JJA.

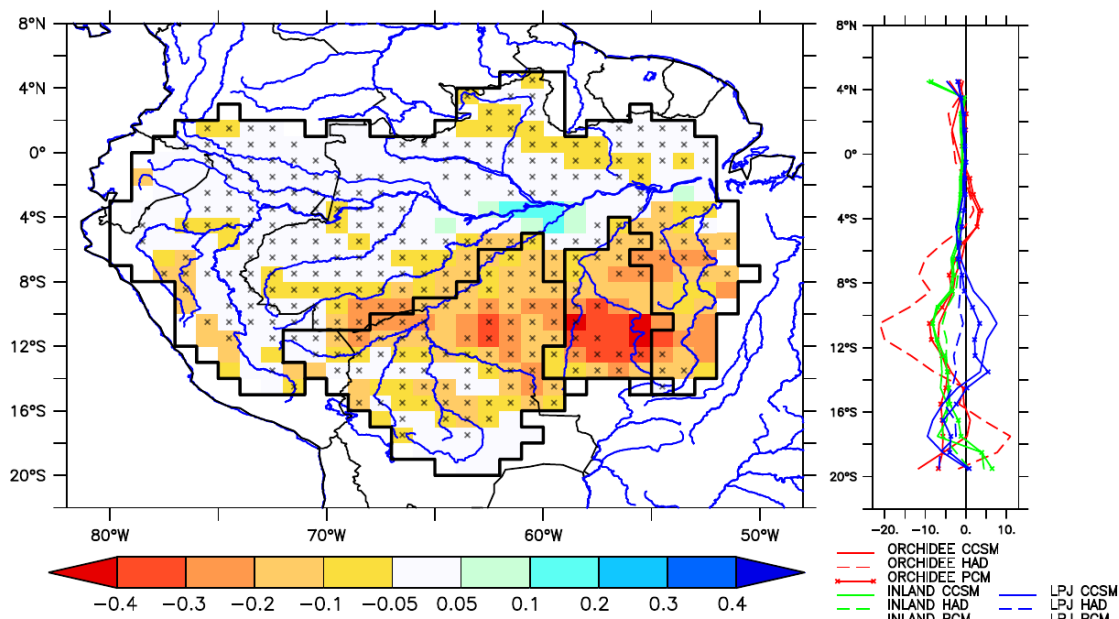


**Figure 4.** Left panel: Simulated spatial change in JJA ET (mm/d) due to SceC2 LCC scenario, from the mean of the 9 DGVMs simulations. Crosses indicate that more than two-thirds of the simulations give an ET decrease on the grid cell. The black lines delineate the Amazon basin and the Madeira (FVA) and Tapajos (ITA) sub-basins. Right panel: Latitudinal relative changes in JJA ET (%) from each of the 9 DGVMs scenarios.

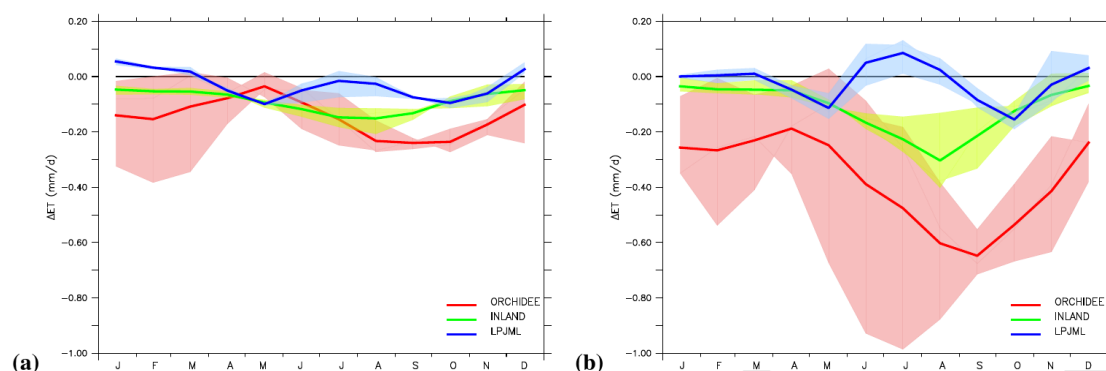


**Figure 5.** Simulated change in seasonal ET (mm/d) due to SceC2 LCC scenario, according to the 3 DGVMs over (a) the Madeira basin (FVA) and (b) the Tapajos basin (ITA). For a given DGVM, the shaded area defines envelopes enclosing the range of plausible climate futures

Deforestation impacts the soil moisture in the southern region. The decrease in ET due to LCC simulated by ORCHIDEE with CCSM forcing leads to a global wetting of the soil during the wet season (from November to March) over the Tapajos basin (Figure 6). During the dry season, which is very marked over this basin (precipitation reaches less than 1mm/d in July), the high climatic demand induces uptakes of water from the soil by the vegetation. In LCC condition, when crops substitute forests, water uptakes occur in shallower soil horizons. When LCC occurs, soil moisture decreases in the first nine soil layers of ORCHIDEE (ie in the first meter of the soil) whereas it increases in the deepest soil layers.

Finally, the deforestation has only little impact on soil water budget over the Amazon basin. However, in the southern region of the basin and mainly in the south-east, the DVGMS simulates a decrease in ET on average over the Madeira and Tapajos, with different magnitudes according to the future forcing used (up to 20% of decrease). This ET decrease affects soil moisture during the dry season and we showed that ORCHIDEE is able to represent the restructuring of the water uptakes by the vegetation in the soil horizons when crops substitute forests.

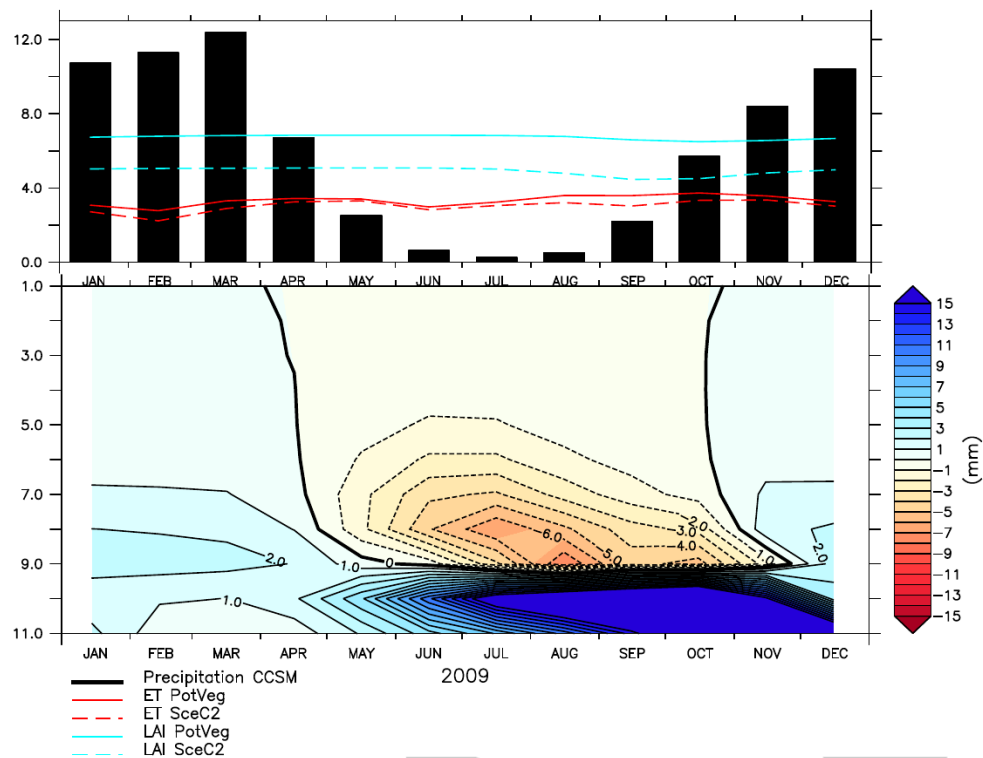


**Figure 6:** Upper panel: Seasonal precipitation (mm/d) from CCSM future forcing and ET (mm/d) and LAI (m<sup>2</sup>/m<sup>2</sup>) simulated by ORCHIDEE over the Tapajos basin (ITA), from PotVeg and SceC2 LCC scenarios. Lower panel: Soil moisture variation (mm) in the 11 soil layers of ORCHIDEE due to SceC2 LCC scenario, for the CCSM future forcing

## 4. Possible effects of climate and land use change on river discharge and functionality of hydropower plants

Within Amazalert WP2, possible effects of climate and LUCC on river discharges and functionality of existing and planned hydropower plants were studied with focus on sub-basin scales (tributaries of the Amazon river), using INPE's distributed hydrological model MHD (Tomasella and Rodriguez, 2014; Rodriguez, 2011), and on wider scale of the whole basin, the global vegetation and hydrology model LPJmL (Rost et al, 2008).

Hydropower is the main source of energy for the Amazonian countries, and in particular Brazil, where it produces over 90% of the electricity (EIA, 2009). The energy consumption in this region has been increasing by almost 40% between 1999 to 2009 (EIA, 2009), and a further increase in energy demand is foreseen. Because the hydropower potential of the water abundant Amazon seems to be inexhaustible, major investments in new hydropower plants are planned (figure 7), especially in the western and south eastern parts of the basin. However, hydropower production depends on river waters in adequate levels to generate energy. It is unclear how changes in climate and land use will affect the hydrological patterns, and therefore the potential energy production of all these planned structures. Moreover, there is a need to systematically assess the potentially negative effects of those structures on both people and ecosystems.

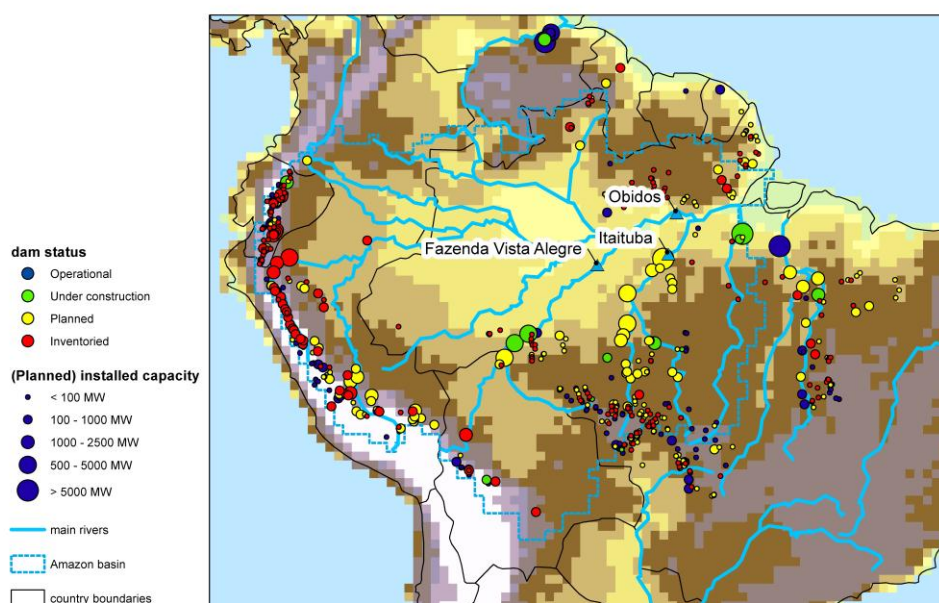


**Figure 7.** Locations, installed capacity and status of planned dams in the Amazon basin. Blue triangles indicate locations of discharge measuring stations on the Madeira (Fazenda Vista Alegre), Tapajós (Itaituba) and Amazon main stem (Obidos) for validation of the LPJmL model and assessment of changes in mean annual cycles of river discharge.

## 4.1. Impacts on sub-basin scales

Hydrological impacts due to climate change affect human activities, such as hydroelectric generation, and should be carefully studied for better planning of water management. Brazil is highly dependent on water resources for several economic activities, particularly for hydropower generation and agriculture (Marengo, 2008). In this context, an increased need for energy to sustain economic growth has boosted governmental plans to expand hydropower in Amazonia. The Investments within the Growth Acceleration Program - PAC (BRASIL, 2013), a governmental plan to promote development, including the construction of hydropower plants, has allocated 45 billion Brazilian Reais (approximately 23 billion dollars) to the Amazon region. The new plants will increase the contribution of the Amazon region to the Brazilian power generation from 10% up to 24% (Empresa de Pesquisa Energética (EPE), 2012). Brazilian strategic interest in the Madeira and Tapajós River basins, important southern Amazon tributaries, and Tocantins River basin, includes the development of hydropower to satisfy the country's growing energy needs and new waterways to boost regional trade and economic development. Figure 8 shows the three sub-basins studied using MHD-INPE.

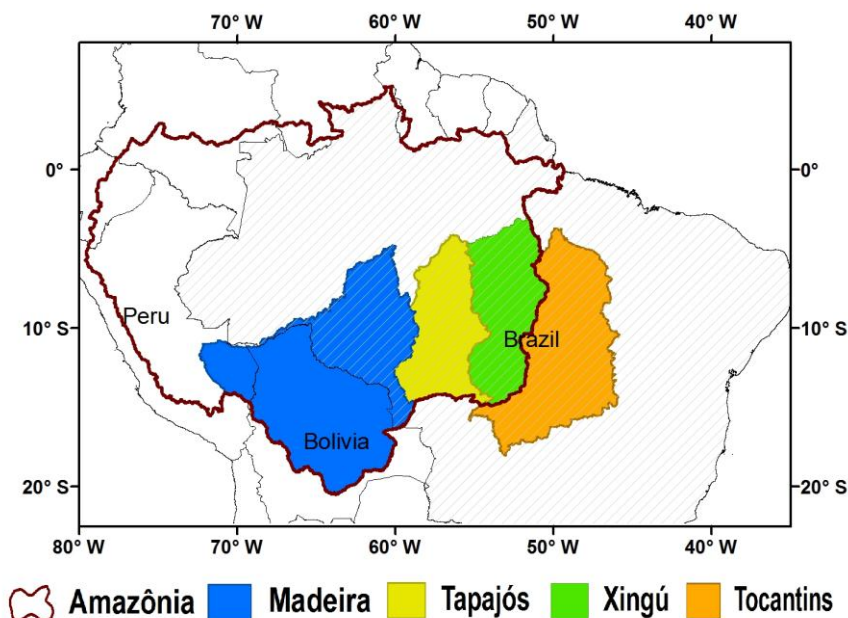


Figure 8: Sub-basins of Amazon tributaries and Tocantins river basin.

### 4.1.1. Sites and Methods Description

#### *Madeira Basin*

With a drainage area of approximately 1,420,000 km<sup>2</sup> across Bolivia (51%), Brazil (42%) and Peru (7%), the Madeira River is one of the most important Amazonian tributary. The Madeira river mean discharge at its mouth to the Amazon is approximately 31,704 m<sup>3</sup>s<sup>-1</sup>, which corresponds to 15% of the Amazon mean discharge. Andean tributaries of the Madeira River drain semi-arid areas of high altitude and areas of tropical humid forest of the

piedmont. The basin mean average rainfall is approximately 1,834 mm year<sup>-1</sup> (Molinier et al. 1996), with a strong spatial variability ranging from 255 mm year<sup>-1</sup> at the station of Caracato (2650 masl) in the Bolivian Andes to more than 3,000 mm year<sup>-1</sup> in stations located at less than 1,500 masl (Espinoza Villar et al. 2009).

### *Tapajós Basin*

The Tapajós basin is an Amazon sub-basin located within Brazilian territory (Fig 8); it has a drainage area of approximately 493,000 km<sup>2</sup>. The Tapajós River accounts for 12.8% of the Amazon drainage area and 10.9% of its average discharge. The main stem of the Tapajós has a length of 1880 km, and its major tributaries are the Juruena and Teles Pires rivers (Agência Nacional de Águas (ANA), 2013). The high soil storage capacity of sedimentary areas allows the continuity of large discharges during the entire year; thus, the seasonal amplitude is minimized. The mean average discharge in the basin is approximately 3000 m<sup>3</sup>/s. The annual rainfall varies between 1800 and 2300 mm; it mainly occurs during the wet season, between October and April.

The upper Tapajós basin is under intense human pressure due to the expansion of agricultural lands in conjunction with the increased demand of irrigation. Several studies have identified that agricultural lands cover large areas of the Tapajós, indicating a significant demand on water resources with a potential to generate water resource conflicts in the medium and long term (Ministério do Meio Ambiente (MMA), 2006).

### *Tocantins Basin*

Tocantins River Basin is the biggest basin totally belonging to the Brazilian territory, with an area of 918.273 km<sup>2</sup>. The altitude of the Tocantins river basin before the union with Araguaia River varies from 200-500 m in the majority of its area, and is higher than 1000 m for upstream basin. The precipitation average of the basin is 1869 mm per year with a maximum of 2.565 mm in the Pará state cost, while the evapotranspiration average is around 1.371 mm/ano (MMA, 2006b). The precipitation regime happens from South to North. The lower total of precipitation occurs in the border of Goiás and the Northeast region, with average of 1mm/month between June and August. The precipitation decrease from West to East, from 1850 mm to 1000 mm/year (MMA, 2006). The Tocantins-Araguaia region is one of the most important Brazilian hydrography region because of its location and hydropower potential of a total of 26.285 MW. The installed hydropower potential of the region totalizes 6981 MW.

### ***Distributed Hydrological Model – MHD-INPE***

The Distributed Hydrological Model of the National Institute for Space Research (MHD-INPE) is a regular grid-cell model that solves a water balance equation (Rodriguez 2011; Tomasella and Rodriguez, 2014); it was developed from the large-scale hydrological model MGB-IPH (Collischonn, 2008) and has been applied in large Amazonian basins (Tomasella and Rodriguez, 2014; Siqueira Júnior et al., 2014). The model generates fluxes in each cell using the approach developed by Tomasella and Rodriguez (2014), which combines elements of Topmodel (Beven and Kirkby, 1979) and a storage capacity probabilistic distribution concept that was used in the Xinanjiang model (Zhao, 1992). Evapotranspiration is estimated from the Penman-Monteith equation and is separated into evaporation of canopy interception as estimated with the model proposed by Gash et al. (1995), transpiration of the

water taken up by plant roots according to Jarvis' model (Jarvis, 1989), and the evaporation from the soil. Each grid-cell is sub-divided into hydrological response units (HRU), and the water balance is solved for each unit. Routing between grid cells is performed according to the Muskingum-Cunge methodology (Garbrecht and Brunner, 1991).

The model uses meteorological data (air temperature, dew point temperature, wind speed, atmospheric pressure, incoming radiation and precipitation) as input data. The drainage network is derived from the basin digital elevation model (DEM). The combination of soil types with land use and land cover change maps are used for defining HRU within each grid cell.

### *Hydrological model calibration and validation*

MHD-INPE model was calibrated against observed discharge data for the 1970-1990 period, using observed meteorological data as input. The performance criteria for the calibration were three different performance indices: Nash-Sutcliffe efficiency (ENS), the Nash-Sutcliffe efficiency of the logarithmic values of discharge (ENSLog) and the relative volume error ( $\Delta V$ ) (Krause et al., 2005; Moriasi et al., 2007). For validation, the performance of the model to simulate the present climate conditions when data from climate models are used as input is evaluated using signatures of the flow duration curves (FDCs) (Yilmaz et al., 2008; Ley et al., 2011).

Model calibration and validation carried out by Mohor et al (2014) and Siqueira Junior et al. (2014) show that MHD-INPE performed well in simulating the historic streamflow data at the gauging stations. Nash-Sutcliffe efficiency (ENS) and the Nash-Sutcliffe efficiency of the logarithmic values of discharge (ENSLog) were acceptable for the purpose of this study. Discharge simulated for historical period (1970-1990), using atmospheric data as input, are also consistent with results obtained from the calibration stage (Mohor et al, 2014; Siqueira Junior et al., 2014).

### *Data*

Vegetation cover was obtained from the RADAM-IBGE (IBGE, 1992) and the PROVEG Project (Sestini et al., 2002), which classify the vegetation map according to SiB classes (Sellers et al., 1986). Yearly information regarding land use and land cover change was obtained from the historical reconstruction by Leite et al. (2011) based on historical census data and contemporary land use classification, considering cultivated areas and both natural and planted pastures in Amazonia. The soil type distribution was extracted from the soil map of EMBRAPA (1980). We assembled meteorological, hydrological and soil data from different sources of Bolivian, Brazilian and Peruvian sources. Geomorphologic information was derived from the Shuttle Radar Topography Mission (SRTM).

### *Climate Projections*

A set of global climate models was used as input for MHD-INPE: MIROC-5 (Watanabe, 2010); CSIRO-Mk3.6.0 (Rotstayn et al., 2010); IPSL-CM5A-LR (Dufresne et al., 2013); and HadGEM2-ES (Collins et al., 2008). We also used dynamically downscaled data from the Atmospheric Model Eta-INPE over South America (Chou et al., 2011). The choice of the models was based on their representations of the main characteristics of the present climate over South America.

These global climate models are part of the Coupled Model Intercomparison Project Phase 5 (CMIP5) (Taylor et al., 2012). The projections are based on the Representative Concentration Pathways (RCP) 4.5 emission scenarios (Thomson et al., 2011). Eta-INPE downscaling uses four members of a perturbed physical ensemble of the HadCM3 model as boundary conditions (Gordon et al., 2000; Collins et al., 2001) for the emission scenario SRES (Special Report on Emissions Scenarios) A1B (Nakicenovic et al., 2000). The Moore protocol used in the Amazalert is also uses the HadCM3 model as boundary conditions. This makes possible the comparison of the results from other models using Moore protocol with MHD results, since the same LUC maps are applied.

The application of the meteorological data from the climate models for hydrological applications has spatial and temporal resolution constraints; bias in the variables' distributions is expected. For the bias correction, we applied a percentile-to-percentile approach based on Bárdossy and Pegram (2011) to the precipitation data, while the other meteorological data were bias-corrected using the Delta Change Approach (e.g., Hay et al., 2000).

#### *Land use change trajectories*

Land use projections performed with LUCME in AMAZALERT were considered in the analyses of Tocantins and the secondary forest was taking into account to evaluate its impact on discharge based on the theory that the evaporative rate of this type of vegetation can be larger than in primary forest (Giambelluca, 2002) .

Additional to the land use projections performed with LUCME, previous projections for land use change, produced by Soares Filho et al. (2006), were also considered in the analyses at the Madeira basin. Land-use and land-cover changes - LUC trends produced by Soares Filho et al. (2006) for the 'business-as-usual' scenario (BAU) suggest contrasting rates of forest cover lost in the Brazilian region of the Madeira basin compared with the Bolivian side. Because the forest conversion to pasture promotes the reduction of evapotranspiration, the impacts of land-use and land cover changes on the hydrology should be considered in this context.

#### *Impacts on Hydrology*

Change in the hydrologic response of the basin due to climate change was assessed through the comparison of the projected long-term average discharges (LTA) and the simulated LTA for the historical period using the different climate projections. The changes in the magnitude of the annual average were calculated as the difference between the projected values and historical values, which were both simulated using the same climate model data.

#### *Impacts on Hydroelectricity*

For the Tapajós basin, we evaluated the impacts of potential shifts in the hydrological regime due to global climate change for the Teles Pires hydropower plant (HPP) (Figure 9). This HPP will be operational in 2015 (EPE, 2013), and it has an expected lifetime of 55 years. It is a run-of-river (ROR) plant with an installed capacity of 1820 MW, a maximum plant discharge of 3919 m<sup>3</sup>/s, a head fall of 59 meters, a minimum flow (MFD) of 560 m<sup>3</sup>s<sup>-1</sup> and a reservoir with a 152 km<sup>2</sup> surface area (ANA, 2011). The Teles Pires plant is located between the outfall of sub-basins "Jusante Foz Peixoto de Azevedo" (11) and "Santa Rosa" (12). The impacts of climate change on hydropower generation were estimated using the

methodology of Vogel and Fenessey (1995), which was developed to study the viability of hydropower ROR plants. In this method, a power duration curve (PDC) was derived from the annual FDC calculated from the median of daily values. From the annual FDC, it is possible to calculate the energy production associated with each discharge to obtain a PDC for a typical (hypothetical) year. The integration of the area under this curve represents the typical (hypothetical) annual energy production (Vogel and Fenessey, 1994).

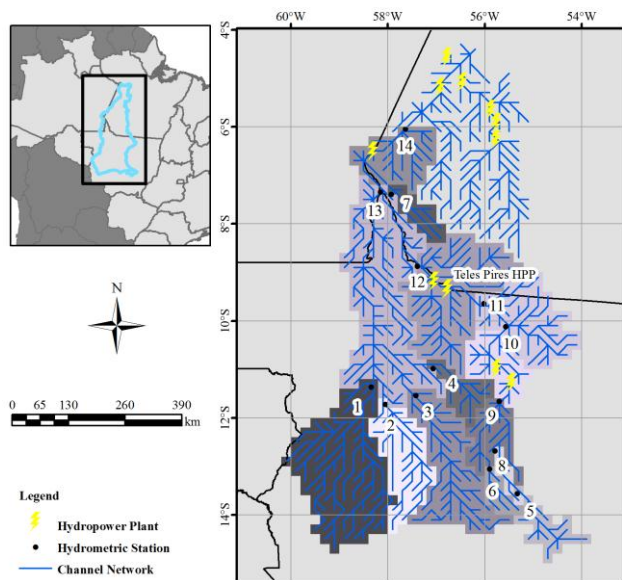


Figure 9: Tapajós basin and the location of Teles Pires HPP.

The same methodology was applied to three ROR hydropower plants at Tocantins:

- 1) Cana Brava. This HPP is operational since 2002, with granting until 2033. It is a run-of-river (ROR) plant with an installed capacity of 450 MW, a head fall of 43.1 meters, a minimum flow (MFD) of 150 m<sup>3</sup>s<sup>-1</sup> and a reservoir with a 139 km<sup>2</sup> surface area. Cana Brava is located at sub-basin “Carolina” (4).
- 2) São Salvador. This HPP has granting to operate until 2023. It is a run-of-river (ROR) plant with an installed capacity of 243 MW, a head fall of 22.84 meters, a minimum flow (MFD) of 102 m<sup>3</sup>s<sup>-1</sup> and a reservoir with a 86 km<sup>2</sup> surface area. The São Salvador plant is located at the sub-basin "Carolina" (4).
- 3) Estreito. This HPP is operational since 2011. It is a run-of-river (ROR) plant with an installed capacity of 1087 MW, a head fall of 18.9 meters, a minimum flow (MFD) of 585 m<sup>3</sup>s<sup>-1</sup> and a reservoir with a 555 km<sup>2</sup> surface area. The Estreito plant is located between the outfall of sub-basins "Carolina " (4) and "Descarreto" (5).

Figure 10 shows the location of the ROR HPP of Tocantins sub-basin.

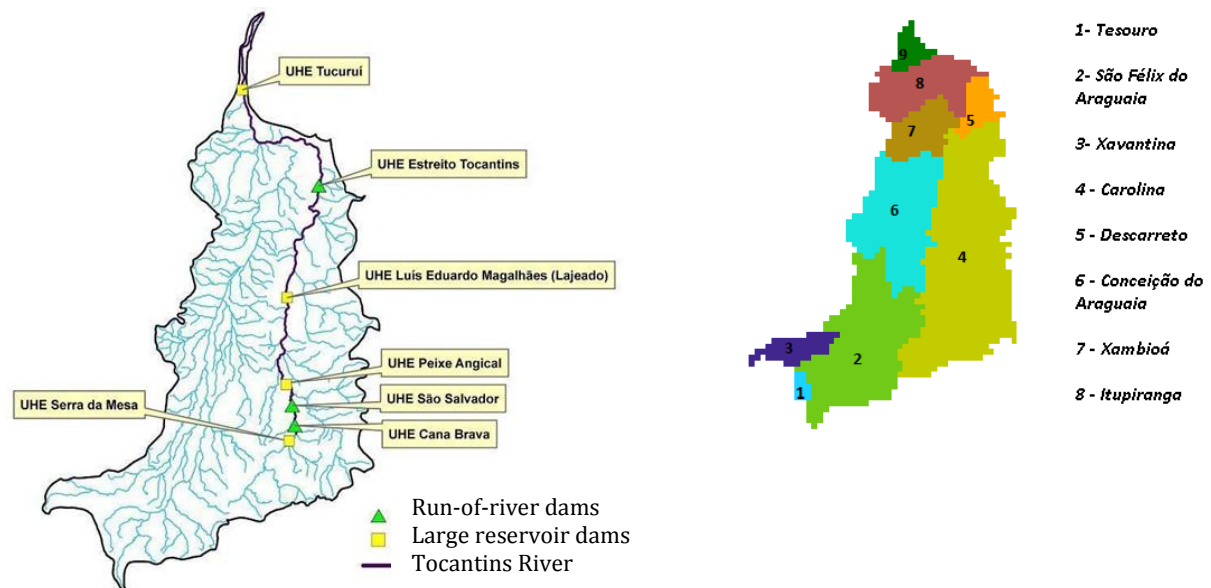


Figure 10: Tocantins river basin and the HPP location (left) and the sub-basins considered for calibration of the MHD model (right).

Within the Madeira River basin, two ROR hydropower plants are already under construction: Santo Antonio and Jirau (Figure 4). We calculated the energy potential generation based on the projected discharges of the grid-cell close to the locations of Santo Antonio run-of-river plant (firm energy capacity of 2,218 MW, net head of 19 m) for both the present climate and projection scenarios. Using the same methodology, we also calculated the energy generation potential for the large reservoir dams of Tocantins: Peixe Angical HPP (firme energy capacity of 450 MW, net head of 24.3 m), Luis Eduardo Magalhães - Lajeado (firme energy capacity of 950 MW, net head of 29 m), Serra da Mesa (firme energy capacity of 1275 MW, net head of 127 m) and Tucuruí (firme energy capacity of 8125 MW, net head of 60.3 m).

As recommended by Paish (2002) we estimated the energy generation potential using the following equation:

$$E_p \text{ [MWm]} = 0.0088 \times H_m \times Q_m$$

where  $E_p$  is the average energy potential [MW];  $H_m$  is the average net head [m], assumed to be constant in all climate change scenarios; and  $Q_m$  is the mean net flow [ $\text{m}^3 \text{s}^{-1}$ ]. The coefficient 0.0088 results from the product of the specific weight of water ( $1.000 \text{ kg} \cdot \text{m}^{-3}$ ), the efficiencies factors of the turbine (0.93) and generators (0.97), the force of gravity ( $9.81 \text{ m s}^{-2}$ ) and the coefficient  $1.10^{-6}$  that converts the average energy in MW.

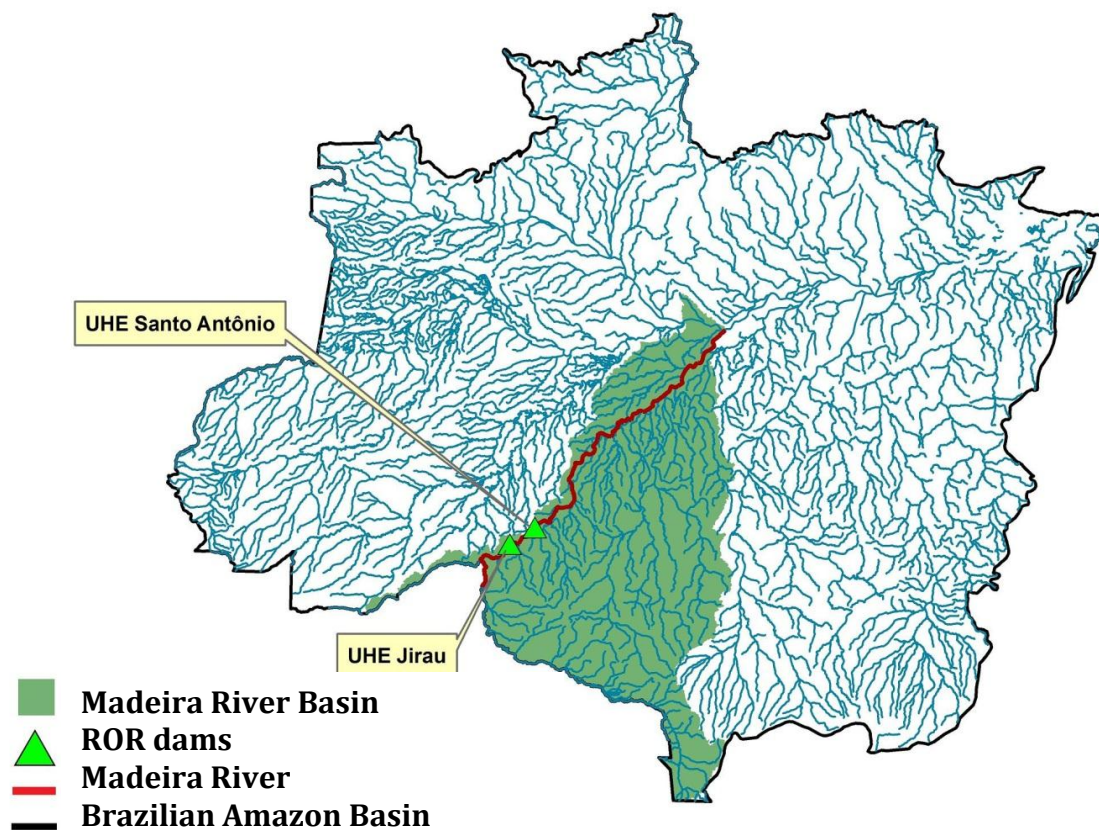


Figure 11: Madeira River basin in Brazilian territory (shaded area) and the ROR HPP location.

#### 4.1.2. Results

##### *Impacts on hydrology*

##### *TOCANTINS*

The Carolina sub-basin, which contains the majority of the hydropower plants of Tocantins river basin, and the Descarreto sub-basin do not presented a significant difference between both A and C1 LUCC scenarios because most of the cover is savanna (Figure 12). LUCC-ME does not count with deforestation of savanna, therefore, the analysis of hydropower generation of those sub-basins will be presented only for scenario C1.

However, the Tucuruí hydropower, which is located at basin's mouth, presented differences between the scenarios (Figure 13), therefore, the analysis of impacts on hydrology and on the hydropower generation of Tucuruí hydropower plant will be presented for both A and C1 scenarios.

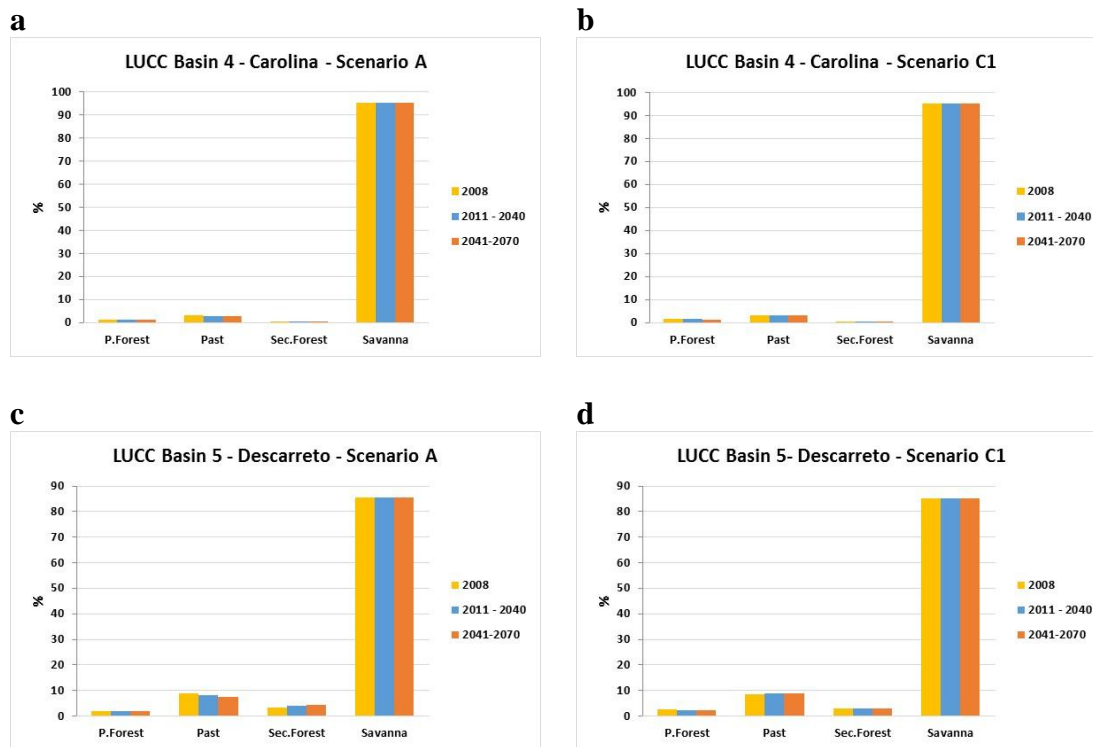


**Figure 12.** Area coverage (%) of different land use types, as projected by LUCCE model, for scenarios A (sustainable, left panels) and C1 (intense deforestation, right panels), for 2 sub-basins within the Tocantins basin: Carolina (a and b) and Descarreto (c and d).

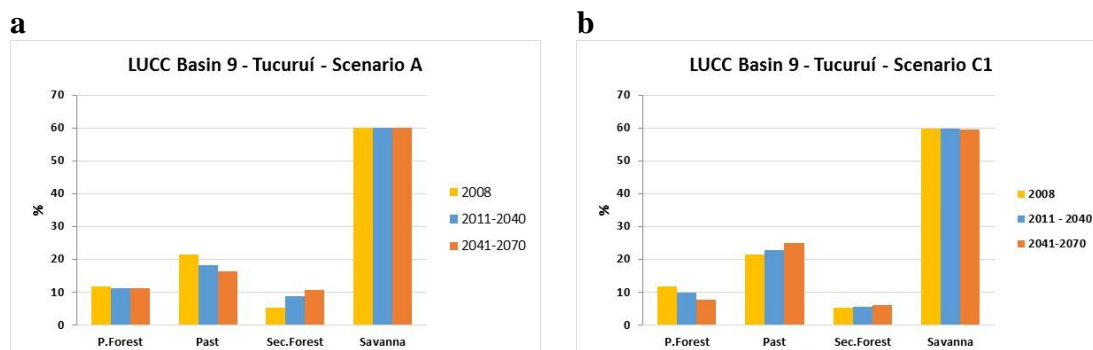


**Figure 13.** Area coverage (%) of different land use types, as projected by LUCCE model, for scenarios A (sustainable, panel a) and C1 (intense deforestation, b), for the Tucuruí sub-basin, located near the mouth of the Tocantins basin.

In the Tocantins basin, climate change impacts on the long-term average discharge at the Tucuruí gauge station show small variability between the CC only and CC+ScenA. In CC+ScenC1, the discharge is slightly higher than on CC and CC+ScenA. This happens because ScenC1 has more deforestation, what lead to a discharge increase (Fig. 14). In figure 14, for simplicity, the baseline used as a reference corresponds to the average of the simulations over the historical period using all climate scenarios of Eta.

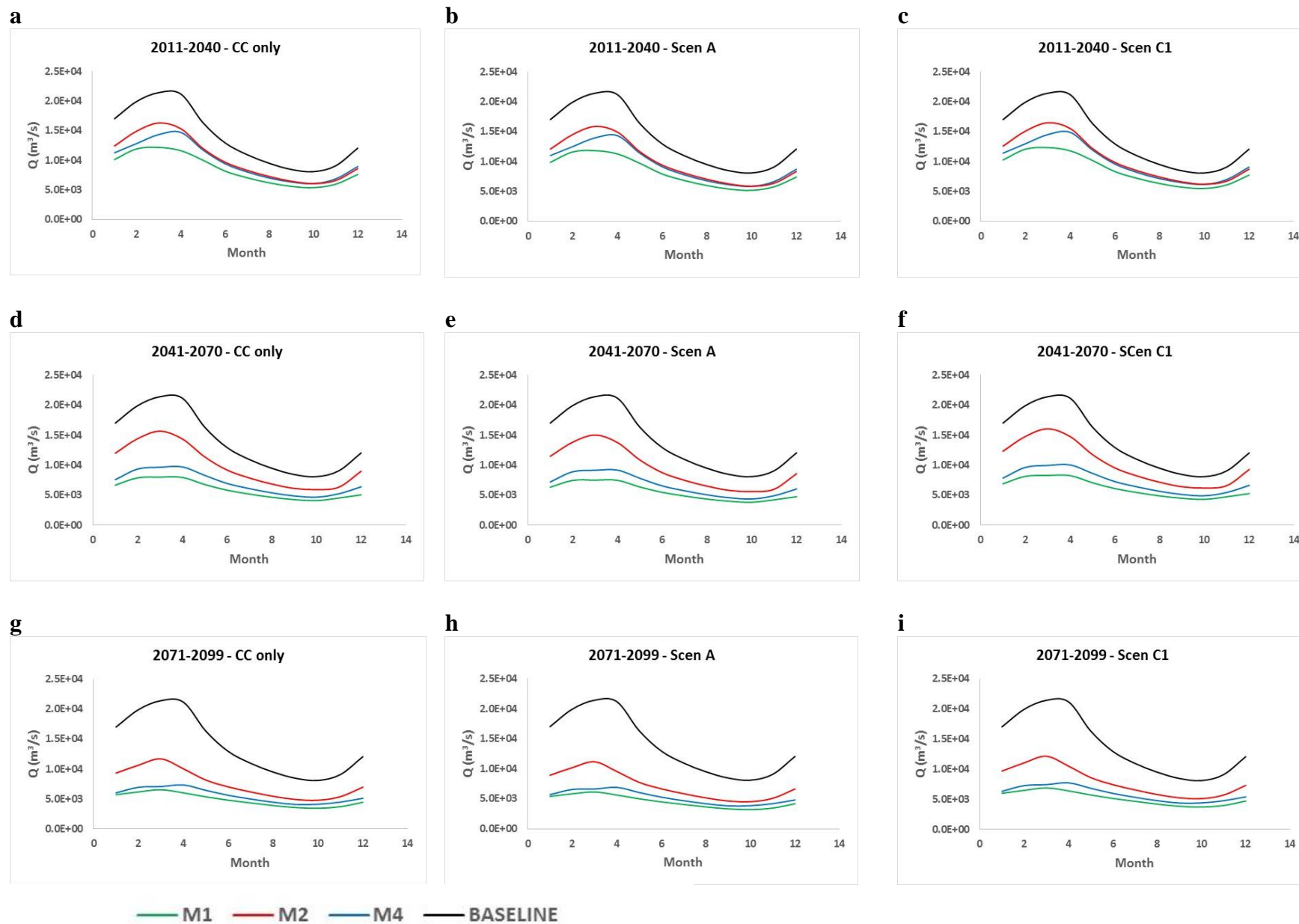


**Figure 14.** Projections of monthly long-term discharges at Tucuruí gauging station, Tocantins basin, for the time slices 2011-2040 (a-c); 2041-2070 (d-f), and 2071-2099 (g-i), considering CC only (left panels), CC+LUCC under sustainable land use scenario A (middle panels) and CC+LUCC under chaotic land use scenario C1. The baseline is the average of the simulations using climate models data in the historical period (1970 to 1990).

## TAPAJOS

In the Tapajós basin, climate change impacts on the long-term average discharge at the Fortaleza gauge station show high variability among the models (Fig. 15). In figure 15, for simplicity also, the baseline used as a reference corresponds to the average of the simulations over the historical period using all climate models. It is worth noting that the largest variations occur in the wet season (JAN-MAY). In general, Eta-INPE members show more variability and broader seasonal amplitudes. However, the IPSL projections produced an increase in the discharge during the wet season.

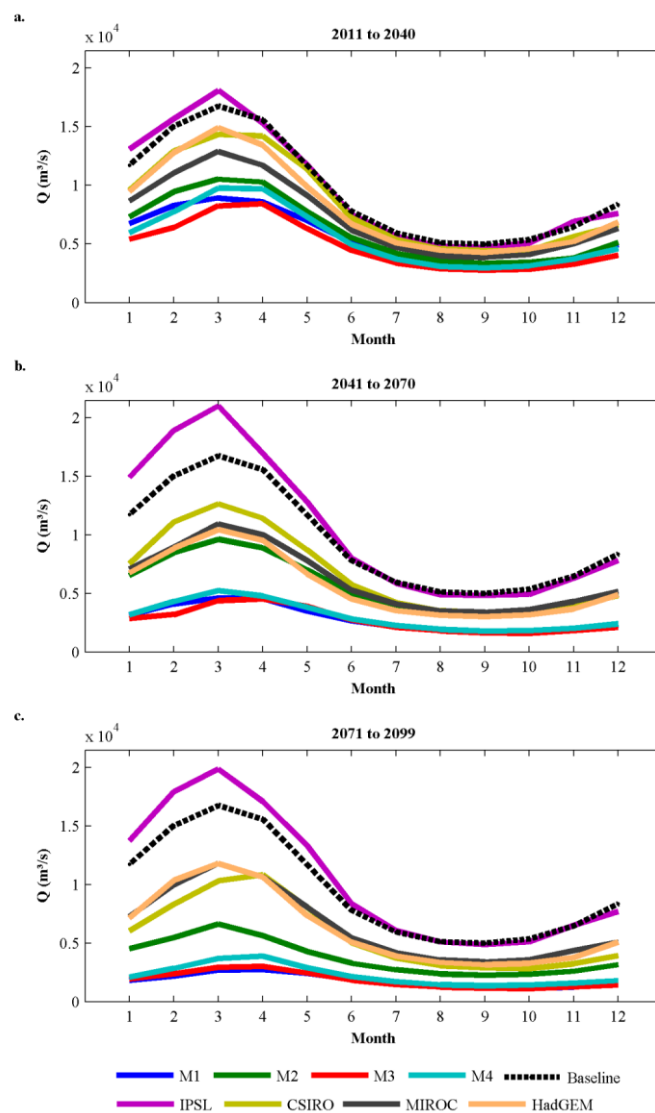


**Figure 15.** Projections of monthly long-term discharges at Fortaleza gauging station, Tapajós basin, for the periods between a) 2011 and 2040; b) 2041 and 2070, c) 2071 and 2099. The baseline is the average of the simulations using climate models data in the historical period (1970 to 1990).

*MADEIRA*

At the Madeira basin, for the sake of simplicity, we show the results for Fazenda Vista Alegre gauging stations, in the lower basin. For clarity, baseline information shown in the figures of this section corresponds to the average of monthly discharge of all climate models for the period 1970-1990, although hydrological impacts were calculated considering the difference between the results for future projections of each model and the simulation of the same model for the period 1970-1990.

Figure 16 shows the mean monthly discharge simulations for the Fazenda Vista Alegre station. Most of the scenarios in the simulations without deforestation (Figure 16a, c, and e) suggested a reduction of discharge along the whole year. However, CSR projections produced higher than the baseline discharges in 2011-2040, while IPS projections discharges were higher in 2041-2070 and 2070-2099.

When LUCC are introduced in the simulations (Figure 16 b, d, and f), IPS, CSR and MR5 models indicated higher than the baseline discharges, with a larger variability among models both in signal and along time-slices. The impacts of LUCC occurred over the entire year. In addition, dry season flows in Fazenda Vista Alegre were, in the case of the M2, MR5, and IPS projections, lower than the dry season flows of the unaltered vegetation scenarios, which appear to contradict the fact that LUCC scenarios are associated with reduced evaporation. This result is due to the occurrence of faster flows in LUCC scenarios compared to the CC scenarios (because of the higher wet season discharges), which cause a more rapid recession.

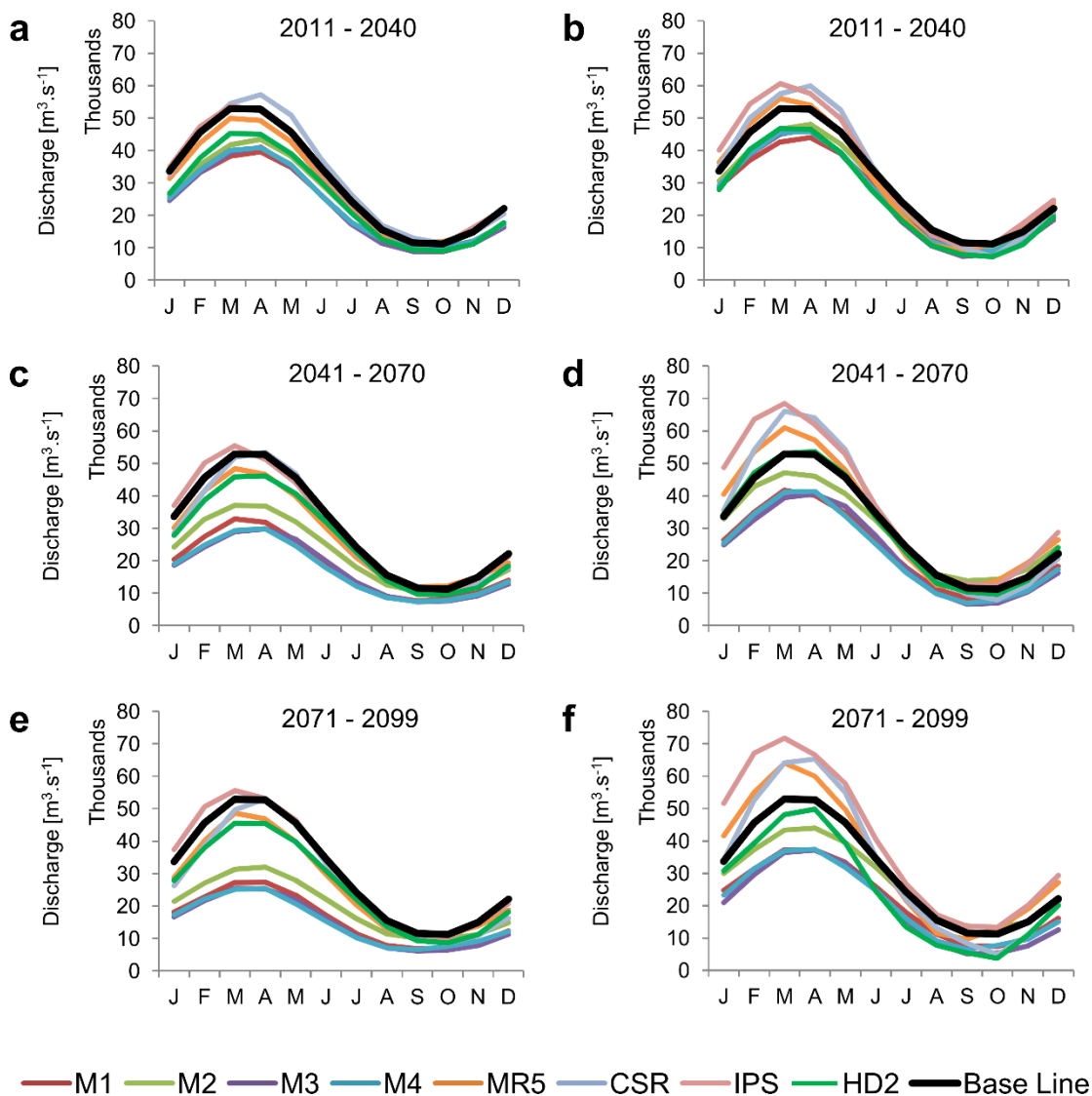


**Figure 16.** Comparison between averaged monthly discharge of all climate models for future projections (the periods from 2011-2040, 2041-2070 and 2071-2099) and the mean monthly discharge of all models for the period from 1970-1990 (referred to as the base line) in the Fazenda Vista Alegre station, in the Madeira’s basin. The left side does not include projected deforestation trajectories; the right side includes projected deforestation trajectories.

*Impacts on Energy Production for large dams*

The change in energy potential presented in this section is the change on energy potential of the one of the future time slice in comparison with historical time slice. The energy potential decreases in all three large hydropower dams in the Carolina and Descarreto sub-basins for both time slices from 2011-2040 and 2041-2070 as a result of CC only, since the basins do not suffer significant LUCC (Figure 17). The higher decrease happened in the M1 scenario (around 50% for the time slice 2011-2040 and around 80% for the time slice 2041-2070). This decrease happened in response to the most significant decrease in the precipitation in comparison with the historical period (around 20% for 2011-2041 and 38% for 2041-2070 on both sub-basins). The Serra da Mesa dam presented a slightly lower reduction on energy

production (around 40% for the time slice 2011-2040 and around 70% for the time slice 2041-2070). The second higher decrease in energy potential happened in the M4 scenario that presented a reduction on energy potential of around 40% for 2011-2041 and 70% for 2041-2070. This decrease happened in response to a reduction in the precipitation of 12% for 2011-2041 time slice and 25% in the 2041-2070 time slice. In the M2 scenario, the reduction on the energy potential was the smallest (30% for the 2011-2040 time slice and 40% for the 2041-2070 time slice) due to the smallest reduction on precipitation (around 10% for 2011-2040 and 12% for 2041-2070).

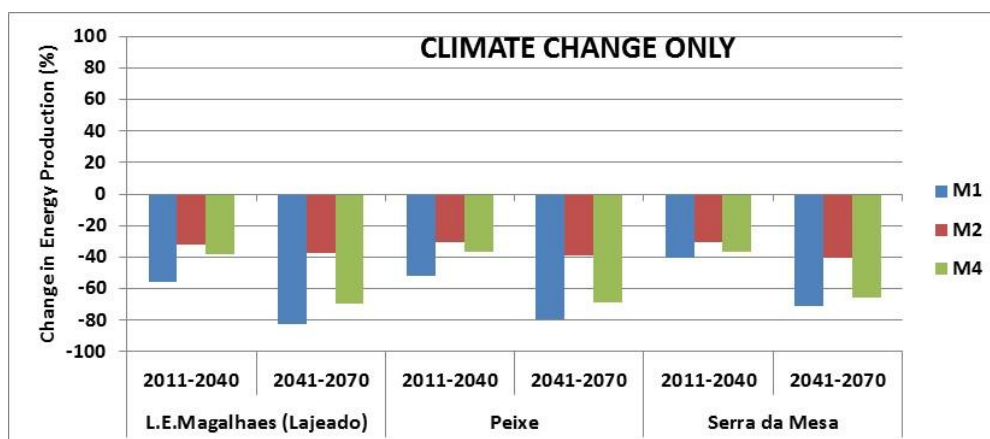


**Figure 17.** Potential impacts on the energy potential at Lajeado, Peixe and Serra da Mesa dams caused by climate change only

The energy potential also decreases in the Tucuruí HPP. The Tucuruí dam area may suffer more pronounced LUCC when compared with the sub-basins Carolina and Descarreto (Figure 13). Therefore, the impacts on the energy potential on this dam are a result of CC and LUCC. The changes caused by CC can be considered similar to that explained for the sub-basins Carolina and Descarreto, since the projected average reduction of precipitation for Tucuruí is similar to the others two sub-basins. We expect a compensation of the decrease in the discharge caused by CC when LUCC is taken into account, mainly because of deforestation. However, the decrease in the energy potential became more pronounced when the scenario A is considered. This happens due to the deceleration of deforestation added to a conversion of pasture into secondary forest, since the primary forest does not change in this scenario (Figure 13). Therefore, this reduction is probably due to the secondary forest transpiration. In order to see impact of the vegetation on the energy potential we fixed the climate change scenario and look at the LUCC only. In Table 1 it is possible to see an increase of evapotranspiration in the scenario A in the future scenarios in comparison with 1970-1990 time slice.

**Table 1:** Change in the ETT in the Tucuruí sub-basin with LUCC scenarios A and C1 in comparison with CC only

Change in ETT TUCURUÍ (%)	CC + LUCC SCENA		CC + LUCC SCENC1	
	2011-2040	2041-2070	2011-2040	2041-2070
CTL	1.02	1.31	0.00	-0.84
LOW	1.17	1.75	-0.55	-1.14
HIG	1.08	1.45	-0.51	-0.93

The compensation on the impact of climate change in the runoff expected by Lucc can be seen in the scenario C1, that has an decrease in primary forest cover leading to an increase in pasture, and the secondary forest and savanna are maintained unchanged. When we consider the Lucc under scenario C1, the energy production decrease is less intense than when only climate change is considered. Nevertheless, the reduction in the energy production in scenario C1 is still high.

Even with around only 10% of secondary vegetation in scenario A the evapotranspiration caused by this type of cover increases in 2% the reduction of energy potential in the 2011-2040 time slice and in 3% in the time slice 2041-2070. When the deforestation increases with the time and the secondary forest is maintained small and unchanged, the energy potential increases only 1% in the 2011-2040 time slice and 2% during the 2041-2070 time slice in comparison with when only CC is considered.

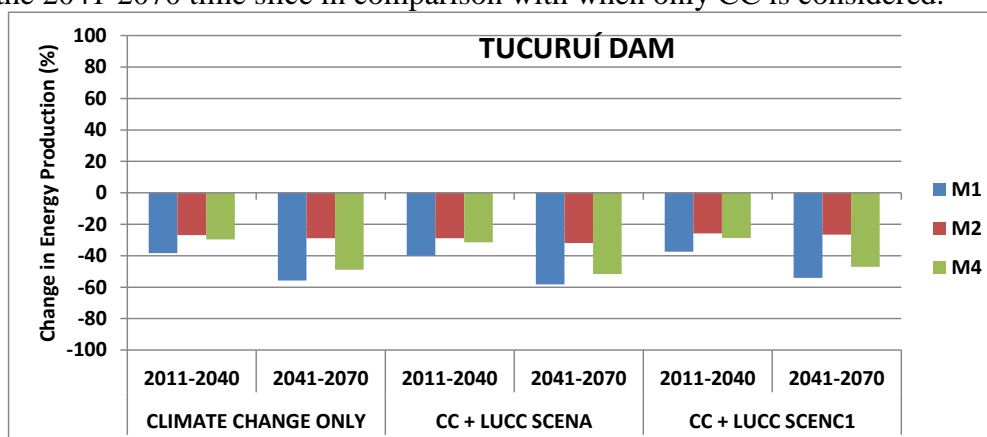


**Figure 18.** Potential impacts on the energy potential at Tucuruí dam caused by climate change only, or combined effects of CC and Lucc under land use scenario A or C1.

This methodology was also applied for run-of-river HPP in Madeira basin. For the Santo Antonio plant, in the Madeira basin (figure 19), the averaged energy potential estimated from the hydrological model simulations using all the climate models was 2,359 MW for the period from 1970-1990.

In terms of impacts of CC, there is no consensus among models. The Eta-INPE model (projections M1-M4) indicated consistent reductions (up to -45% by 2099) of energy potential, whereas the remaining projections showed less important effects with mixed signals. For instance, the CSR projection suggests an increase of 12% for the period from 2011-2040. Including Lucc in the projections, reductions in the M1-M4 integrations are reduced, whereas the other projections indicate increases of up to 38% (IPS) for the period from 2071-2099.

Decreasing energy potential in the M1-4 projections was related to the reduction of discharges during the whole year due to CC effects, which are largely counterbalanced by Lucc effects. In MR5, CSR, IPS and HD2 projections, on the other hand, wet and dry season discharges changes due to CC have opposite signals, which resulted in lower than the baseline annual discharges and, then, in the energy potential. Under Lucc effects, both, higher and lower discharges increased, resulting in a more consistent change in the energy potential in those projections.

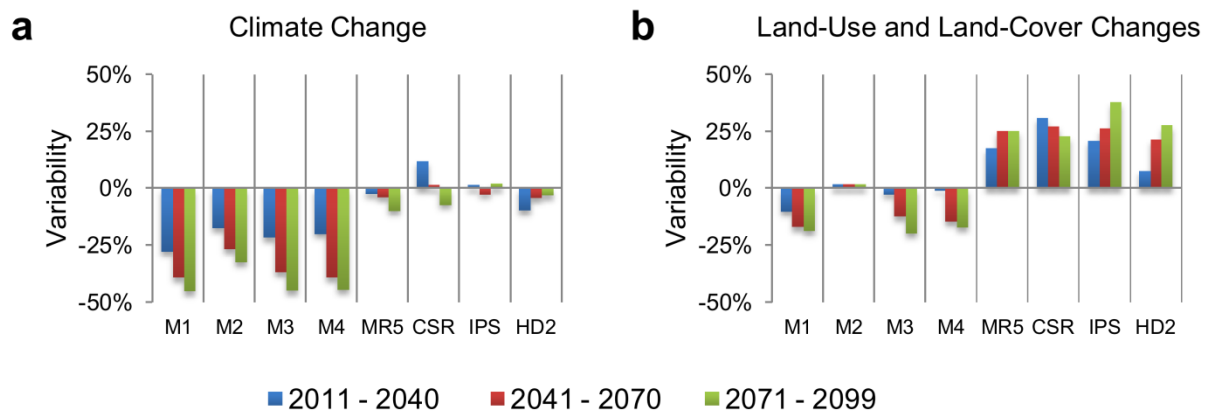


**Figure 19.** Potential impacts on the energy potential at the Santo Antonio dam caused by climate change (a) and climate change combined with land-use and land-cover change (b).

### *Energy Production for Run-of-River dams*

In this section the typical power duration curves for hydroelectric generation at the Teles Pires, in the Tapajós basin; and Cana Brava, São Salvador and Estreito, in the Tocantins basin HPPs will be presented considering the median values during 2041-2070 by the end of the HPP lifetime. The baseline in the historical period represents the PDC of the historical period (1970 to 1990) obtained using observed data as input. The baseline for the 2041-2070 period represents the average of the PDCs obtained using climate models data as input for hydrological model integrations.

Provided the MFD does not change until 2070, the most critical projection/scenario indicates that between 2041 and 2070 the Teles Pires plant should not be operating 59% of the time because the MFD should not be reached (figure 20). The most critical projection for Tapajós, Eta-INPE member M3 indicates a production of  $1.7 \times 10^6$  MWh/year between 2041 and 2070, which is 82% lower than the hypothetical production of  $9.6 \times 10^6$  MWh/year simulated for the historical period. M3 projects that, by the end of the century, the HPP may reach 292 days/year (80%) of idle time and the annual production may fall by 92%. However, the IPSL model projection, which indicates an increase in precipitation, results in a reduction of 3% in the annual production for the period of 2041-2070 and an idle time of 16 days/year (Fig. 20).

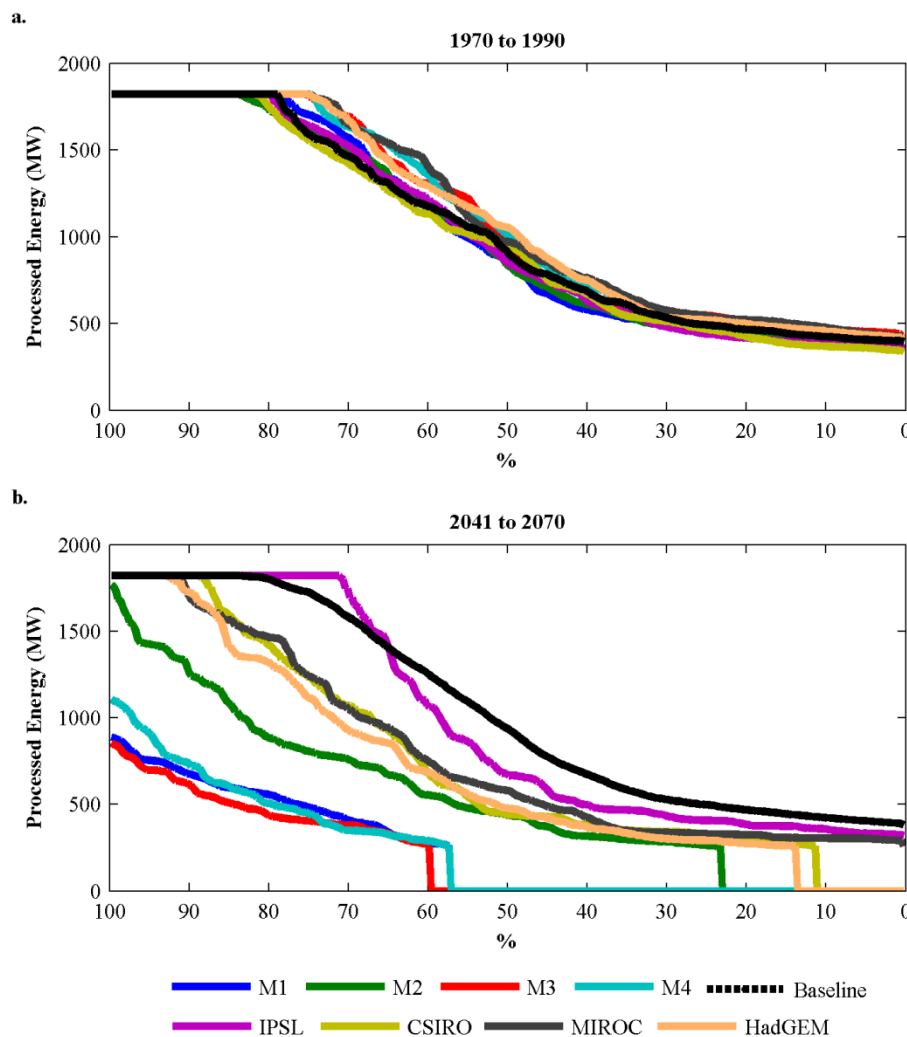


**Figure 20.** Annual Processed Power Duration Curves based in median daily values, at Teles Pires HPP site, for the periods between a) 1970 and 1990, b) 2041 and 2070. The plant's installed capacity is 1820 MW. The baseline in (a) is the PDC of the historical period (1970 to 1990) obtained using observed data as input, in (b) is the average of the PDCs obtained using climate models data as input for hydrological model integrations.

As already shown in the discussion for large dams, in the sub-basins 4 and 5 of Tocantins, the impact on runoff is due to CC, therefore, only CC is shown. The most critical projection/scenario (M1) indicates that Estreito is the plant that suffered the highest impact on reducing time of operation, being not operational 77% of the time. The second more affected plant is São Salvador that should not be operating 65% of the time during the last time of its lifetime. Cana Brava should not operate during 59% of the time in this period (Figure 21). In terms of impact on energy production per year, Estreito PP's production between 2041 and 2070 is  $5.2 \times 10^5$  MWh/year, which is 87% lower than the hypothetical production of  $3.96 \times 10^6$  MWh/year simulated for the historical period for this PP. Cana Brava presented the second higher reduction on the production per year, 85% that represents a drop from  $2.16 \times 10^6$  MWh/year for hypothetical production in the historical period to  $3.2 \times 10^5$  MWh/year in the 2041-2070 time slice. Finally, São Salvador presented a production of  $2 \times 10^5$  MWh/year for the the 2041-2070 time slice that represents a reduction of 83% on the hypothetical production of  $1.2 \times 10^6$  MWh/year.

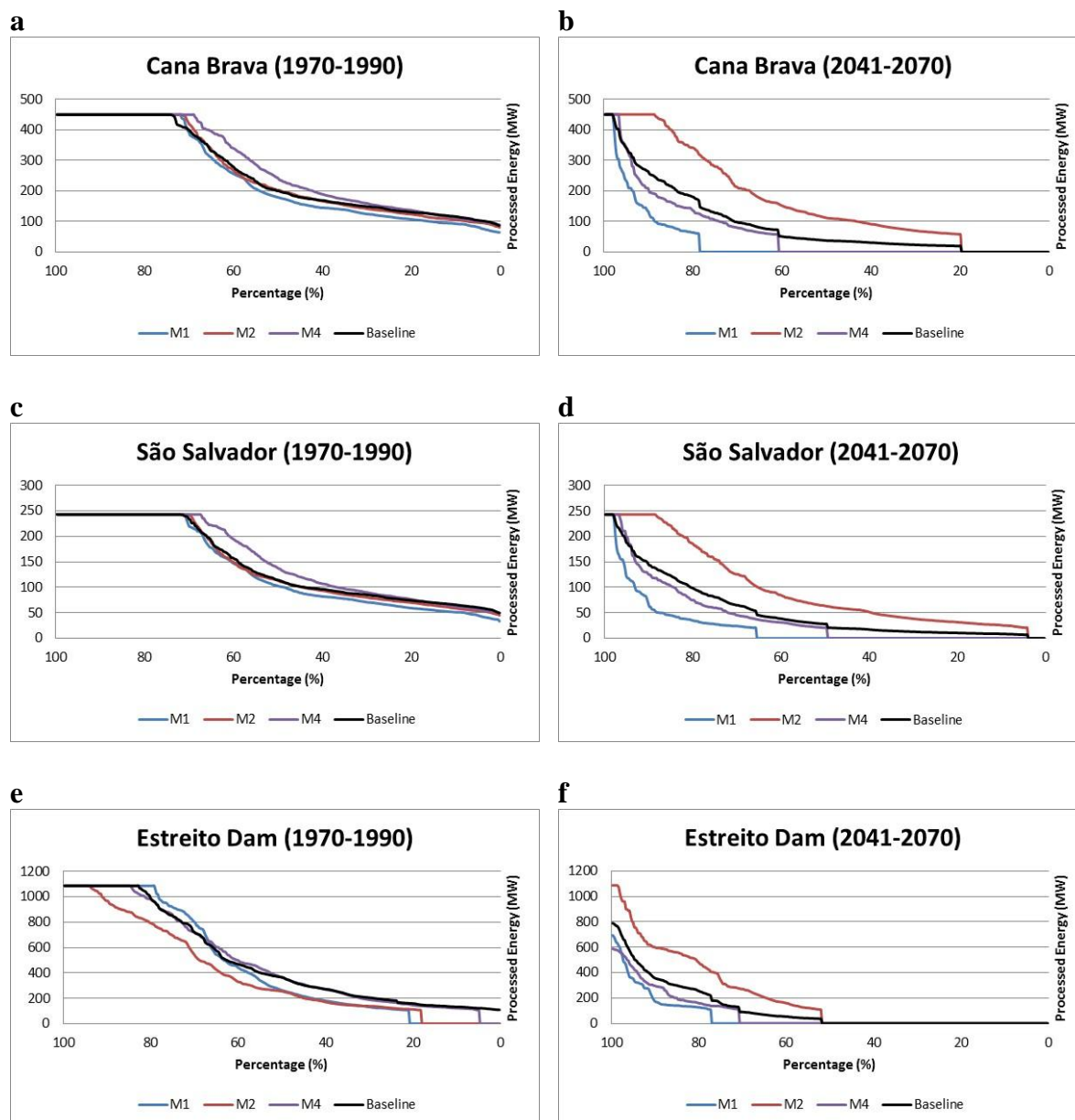


**Figure 21.** Annual Processed Power Duration Curves based in median daily values, at Tocantins run-of-river HPPs, for the periods between 1970 and 1990 (a.1, b.1 and c.1), and 2041 and 2070 (a.2, b.2 and c.2). The plant's installed capacity are 450 MW for Cana Brava, 243 MW for São Salvador 1087 MW for Estreito PPs. The baseline in (a) is the PDC of the historical period (1970 to 1990) obtained using observed data as input, in (b) is the average of the PDCs obtained using climate models data as input for hydrological model integrations

### 4.1.3. Conclusions

Climate change is expected to impact river discharges in the Amazon basin. Since many climate models project substantial decrease in rainfall, especially in South and Southeast of the basin, hydrological model simulations project decreases in discharge accordingly. However, combination of climate change and land use / land cover change may counterbalance this effect.

In the Madeira basin, climate change projections by most models produced a reduction of discharge along the whole year in future time slices, with a consequent reduction

in potential energy production, but this reduction was largely counterbalanced by LUC effects. In some models, however, (MR5, CSR, IPS and HD2), wet and dry season discharges changes due to CC have opposite signals, which resulted in lower than the baseline annual discharges and, then, in the energy potential. Under LUC effects, both, higher and lower discharges increased, resulting in a more consistent change in the energy potential in those projections.

For the TOCANTINS basin, the MHD model was run including LUCME simulations that include the secondary forests, which provided an opportunity to analyse how the recovery of forest cover can also influence discharge and hydropower generation. The changes caused by CC and deforestation were found similar to that obtained for Madeira basin, with a lower decrease in the discharge caused by the CC when LUC of ScenC1 is taken into account, mainly because of deforestation. However, the decrease in the energy potential in the basin may again become pronounced when the scenario A is considered. This happens due to the deceleration of the deforestation added to a conversion of pasture into secondary forest, since the primary forest changes little in this scenario.

Considering that the results presented in this work do not include scenarios for water consumption, it follows that the reduction found on the potential energy production can be further exaggerated. Despite the high variability among the model integrations, the annual energy production is likely to decrease until the end of the century for the analyzed projections under the current HPP design. Although the IPSL scenario in Tapajós points to an increase in rainfall, this is not reflected in the annual production because the constraint is given in terms of plant capacity.

## **4.2. Basin-wide Impacts**

This section presents analyses of hydropower dams at the Amazon basin scale using LPJmL simulations created by forcing LPJmL with observed climate (Sheffield et al, 2006), under potential natural vegetation, performed by WP2 partners PIK and ALTERRA. The objective of this study is therefore twofold. The first is to assess the impact of climate change and land use change on the production capacity of operational and planned hydropower plants and the second to evaluate the potential impacts of operational and planned hydropower plants on downstream ecosystems and ecosystem services.

### **4.2.1. Effects of climate change and land use change on discharge**

We used the global vegetation and hydrology model LPJmL (Rost et al, 2008) to calculate the effects of climate change and land use change on the future hydrology of the Amazon (figure 22). Subsequently, the model was driven with climate scenarios from 3 global climate models for the AR4 SRES A2 scenario (HadCM3, PCM and CCSM) combined with 3 land-use scenarios, representing different levels of deforestation (Aguilar et al, 2012).

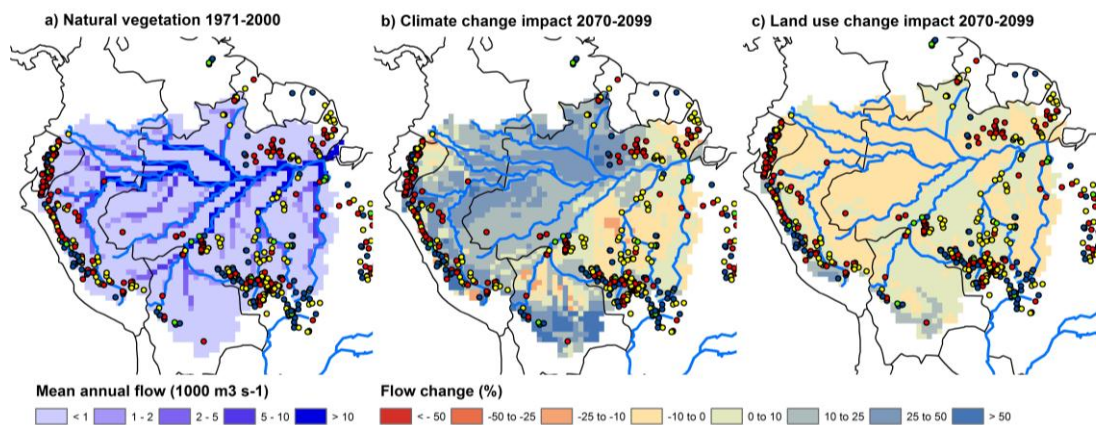


**Figure 22.** a) Mean annual flow calculated with LPJmL forced with observed climate data (Sheffield et al., 2006) under potential natural vegetation. b) projected changes in mean annual flow for 2071-2100 relative to 1971-2000 averaged for three GCMs (HadCM3, PCM and CCSM) for the SRES A2 emission scenario under potential natural vegetation, and c) projected changes in mean annual flow due to land use change (scenario C2 – extreme deforestation) relative to potential natural vegetation. Dots represent locations of operational and planned dams (see figure 7).

From figure 22, we observe that two contrasting patterns are projected for the Northern and the South-Eastern parts of the basin. The major part of the Northern tributaries will experience an increase in average annual streamflow, however decreases in streamflow are expected in the South Eastern part of the basin, where many new hydropower plants are planned (see fig 7). Still, according to these simulations, changes in land use from forest to agricultural land will only have small effects on mean annual discharge (fig 22.c).

#### 4.2.2. Effects of changes in discharge on hydropower generation

We analysed projected changes in mean annual flow at the locations of operational and planned hydropower generation plants (figure 23). Most of the planned hydropower plants will be located in regions where increases in mean annual streamflow can be expected, although over 20.000 MW installed capacity is planned on locations with projections of decreasing streamflow.

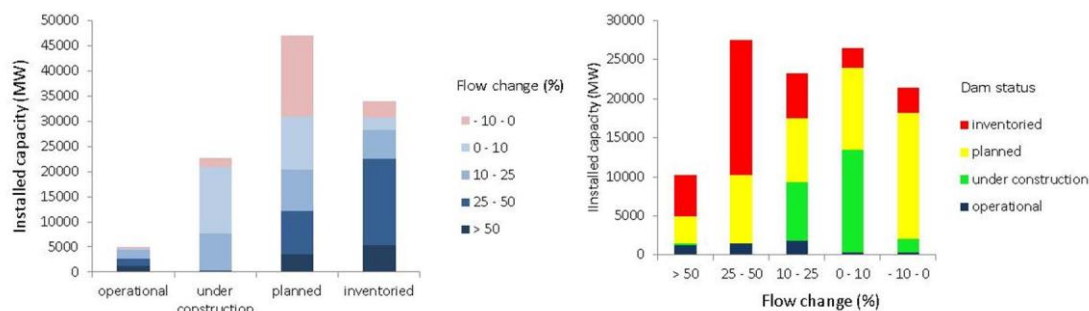


**Figure 23.** Total operational and planned installed capacity in hydropower plants with projected changes in mean annual flow for 2071-2100 relative to 1971-2000.

Based on figure 23, one could therefore conclude that most of those hydropower plants will be able to achieve the planned energy production levels, and eventually even more because of possible increases in discharge. However, more detailed analysis would be necessary, as the achievable energy production will depend on the type of hydropower plant (run-of-the-river or dam with reservoir) in combination with the (changes in) intra- and interannual variability in streamflow.

Energy production in run-of-the-river hydropower plants - that are typically built at locations with high elevation differences but little streamflow - are vulnerable during low flows when minimum levels are required in order to divert the water and keep turbines working. Further, any streamflow above the maximum capacity of the turbines will not be used.

Hydropower plants that consist of big dams with reservoirs, are typically built at lower elevations, with less elevation differences but large volumes of water flowing through. These plants often have a larger capacity than run-of-the-river hydropower plants. Because intra-annual variations in streamflow can be moderated by the reservoir lake, production in these plants is less vulnerable to intra-annual variation. However, those plants are more vulnerable to interannual variations in streamflow when the reservoir in a dry year might not fill up to the level required for ensuring reservoir outflow –and therefore energy production– during the period ahead.

#### **4.2.3. Effects of hydropower generation on downstream ecosystems**

Although an enormous increase in hydropower production can be beneficial for the energy security in the Amazon countries, potential negative effects on people and ecosystems need serious attention and systematic assessment. In order to make a first estimate of the extend of the downstream effects of all planned structures, we implemented all planned hydropower dams in the reservoir module of LPJmL (Biemans et al., 2011) (figure 24).

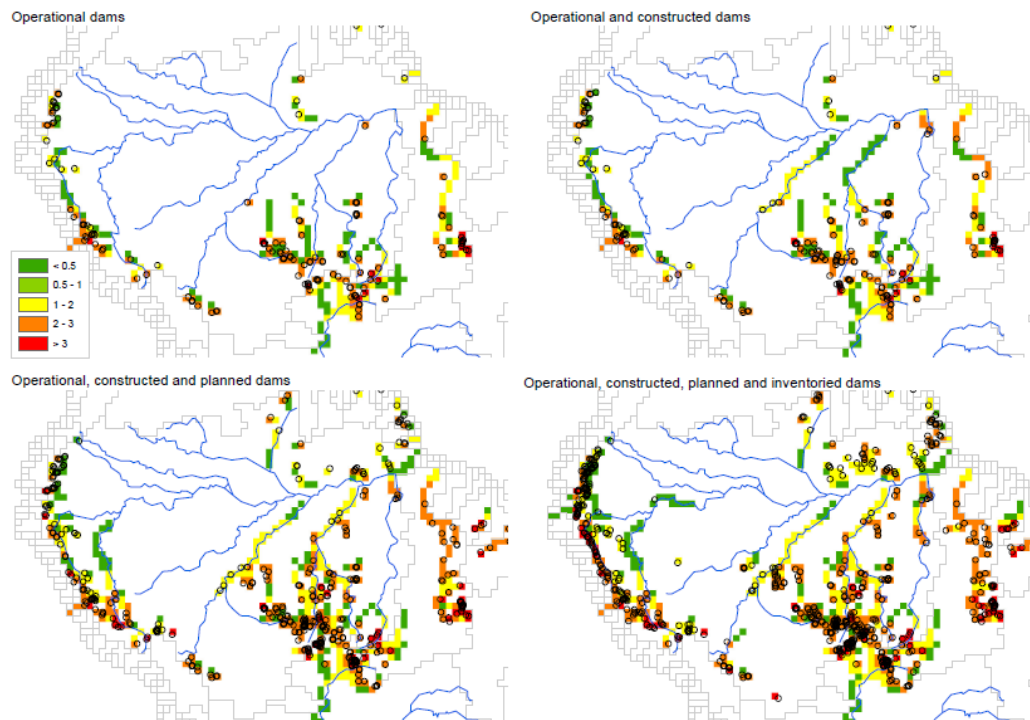


**Figure 24.** Downstream effects of hydropower dams expressed by the Amended Annual Proportional Flow Deviation (AAPFD). The AAPFD is an indicator for the level of modification of a river system compared to its natural conditions (for explanation, see Biemans et al, 2011).

Figure 24 shows that large parts of the Amazon, amongst which the Madeira and Tapajos (see figure 8), will be affected by the enormous constructions foreseen, and that impacts will be felt far downstream of the dams. This will have adverse effects on ecosystems that are depending on the natural variability and temporal inundation of the river.

#### 4.2.4. Discussion and conclusion

Few remarks regarding the simulations of future discharge are to be made. First, we used only 3 GCMs and one emission scenario for the climate forcing. Including more GCMs in the analysis would increase the robustness of the result. Second, we only used one hydrological model to assess changes in discharge, whereas including multiple models would be beneficial. Third, we used a combination of climate forcing and land use change patterns that were not consistent. Therefore, the feedback of deforestation on climate that can have a drying effect is not included in this analysis.

In order to make better estimates on the effects of climate and land use changes on the actual production capacity of the hydropower dams, more information is needed regarding the type of hydropower planned (run-of-the-river or dam with reservoir), and the changes not only in mean annual streamflow, but also intra- and interannual variability. In order to better assess the impact of new structures on downstream streamflow, more information is needed on the volume of the planned reservoir. Finally, further analysis with improved indicators is needed to understand effects of dams on aquatic ecosystems downstream.

## 5. Effect of climate and land use change on average and extreme flows in the Amazon River basin - A scaling approach

There is a fundamental need to understand the variability of average and extreme river flows (floods and low flows) at a broad range of space-time scales. Amazonia is the best laboratory for testing new theories to tackle the problem of Prediction in Ungagged Basins (PUB). Global environmental change (climate change, land use change, resources extraction) is significantly affecting the space-time dynamics of the hydrologic cycle. It is critical to understand how these conditions are affecting the behavior of average and extreme river flows.

In this section, we present analyses performed using the statistical scaling approach proposed by Poveda *et al.* (2007), by linking the long-term water balance equation ( $\bar{Q} = A[\bar{P} - \bar{E}]$ ) with the theoretical framework of statistical scaling. Using the traditional quantile method (Chow, 1951), extreme river discharges ( $Q_p$ ) of different return periods ( $Tr$ ), can be estimated as:

$$Q_p(Tr) = \mu_{Qmax} + k(FDP, Tr)\sigma_{Qmax} \quad \text{where} \quad (1)$$

$$\mu_{Qmax} = \alpha_1 \bar{Q}^{\theta_1} = \alpha_1 [A(\bar{P} - \bar{E})]^{\theta_1} \quad (2)$$

$$\sigma_{Qmax} = \alpha_2 \bar{Q}^{\theta_2} = \alpha_2 [A(\bar{P} - \bar{E})]^{\theta_2} \quad (3)$$

### 5.1. Data

**River Flows:** 138 river discharge gauging stations with more than 20 years of daily and monthly data, from ANA and ORE-HYBAM monitoring network (Figure 25).

#### Precipitation:

Source	Period	Resolution	
		Spatial	Temporal
TRMM	1994-2012	0.25° x 0.25°	Monthly
ORE-HYBAM	1975-2009	1.00° x 1.00°	Daily
SHEFFIELD	1970-2008	1.00° x 1.00°	Sub-Daily

#### Evapotranspiration:

Source	Period	Resolution	
		Spatial	Temporal
GLEAM	1994-2012	0.25° x 0.25°	Monthly
MPI	1975-2009	1.00° x 1.00°	Daily
MODIS	1970-2008	1.00° x 1.00°	Sub-Daily
All AMAZALERT Models	1970-2008	1.00° x 1.00°	Monthly
INLAND (Scenarios A & B)	2009-2050	1.00° x 1.00°	Monthly

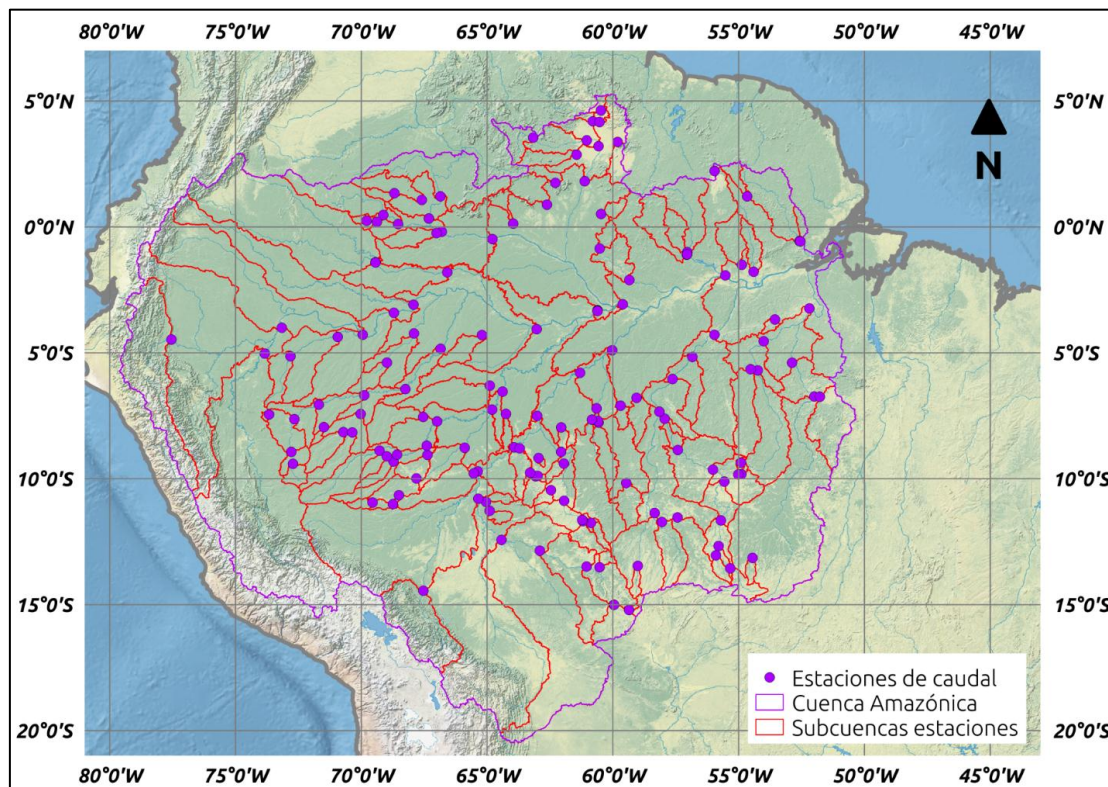


Figure 25. Location of river gauging stations use in the statistical scaling approach

## 5.2. Water Balance Assessment – Present (1970-2008)

The long-term water balance equation was solved at all river gauges (138) sub-basins using all  $P$  and  $E$  datasets described in section 4, and compared with the historical mean river flows. Some of these results are shown in Figure 25. Certain combinations of  $P$  and  $E$  datasets produce the “best” closure of the long-term water balance estimation for present scenarios.

$$Q_m = (\bar{P} - \bar{E}) \cdot A \quad (4)$$

Noting that the only  $P$  dataset that will be “traceable” in future scenarios is Sheffield’s; ORCHIDEE E combination exhibits the lowest errors in the closure of the long-term water balance.

### 5.3. Statistical Scaling and Water Balance - Present (1970-2008)

Relationships between long-term water balance and extreme flows (maximum and low flows) is explored through the framework of statistical scaling ((1 to (3)). Results are shown in Figures 26-28 and Table 2. Extreme river flows (floods and low flows) in the Amazon River basin (and its main sub-basins) exhibit simple scaling with drainage area as scaling parameter.

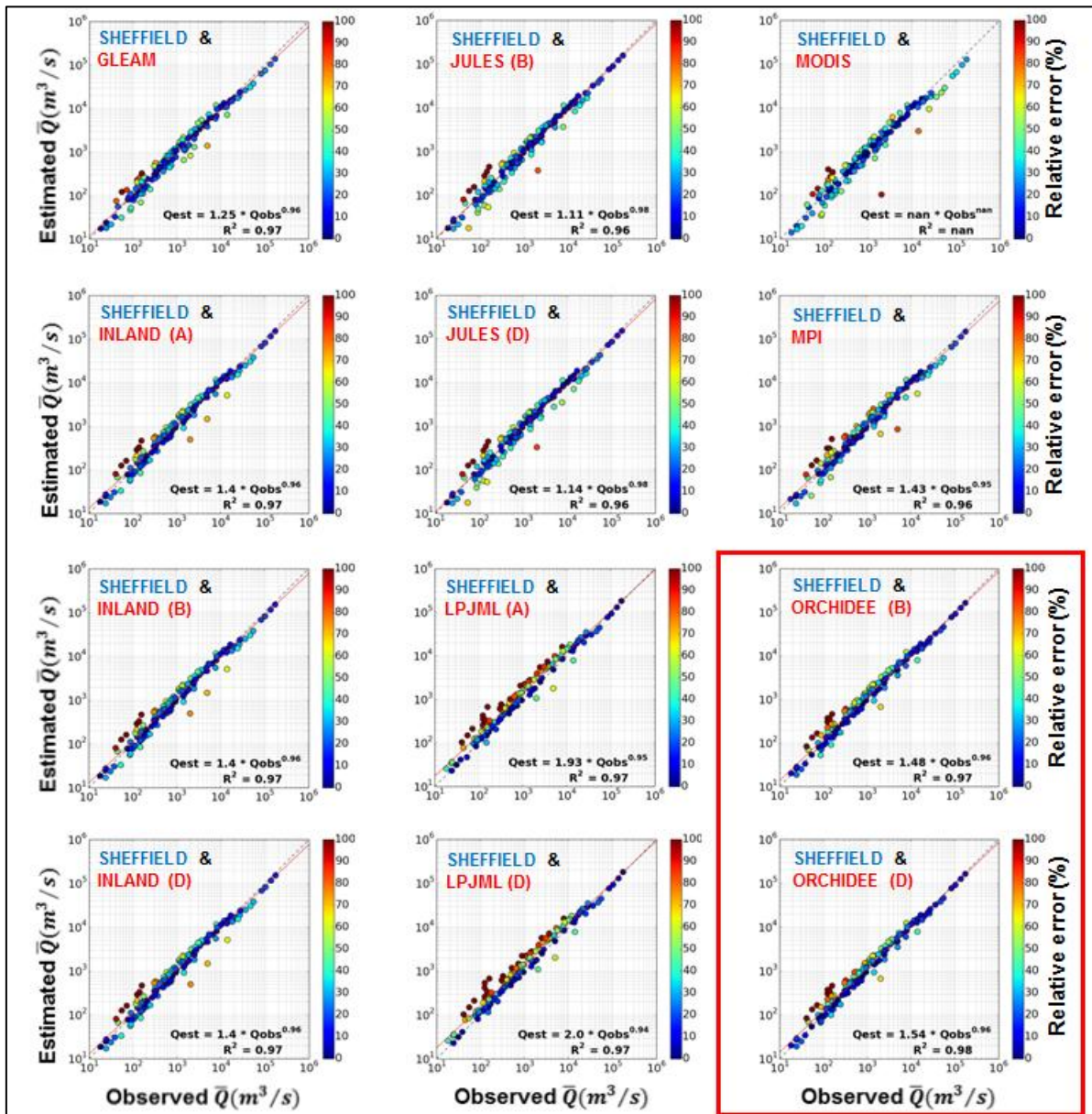
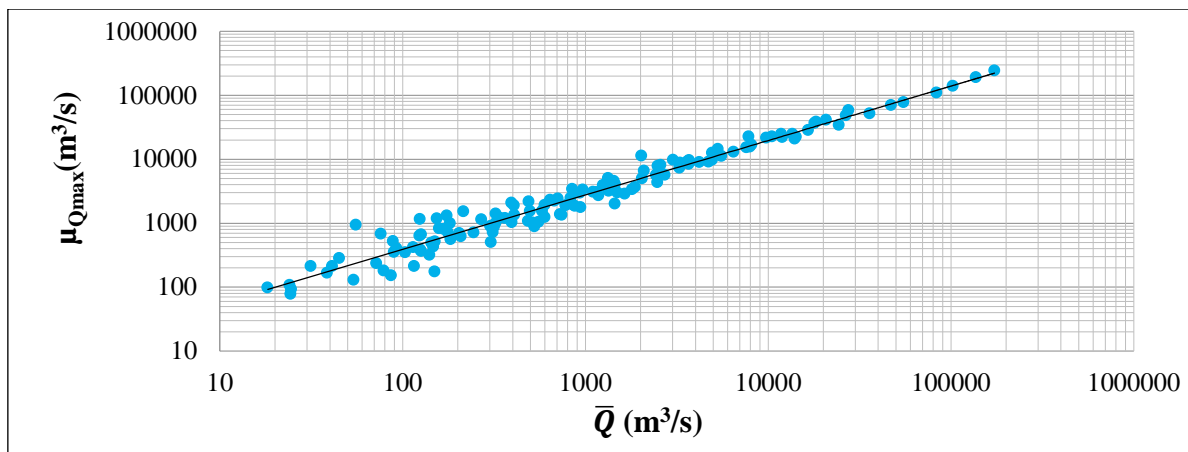
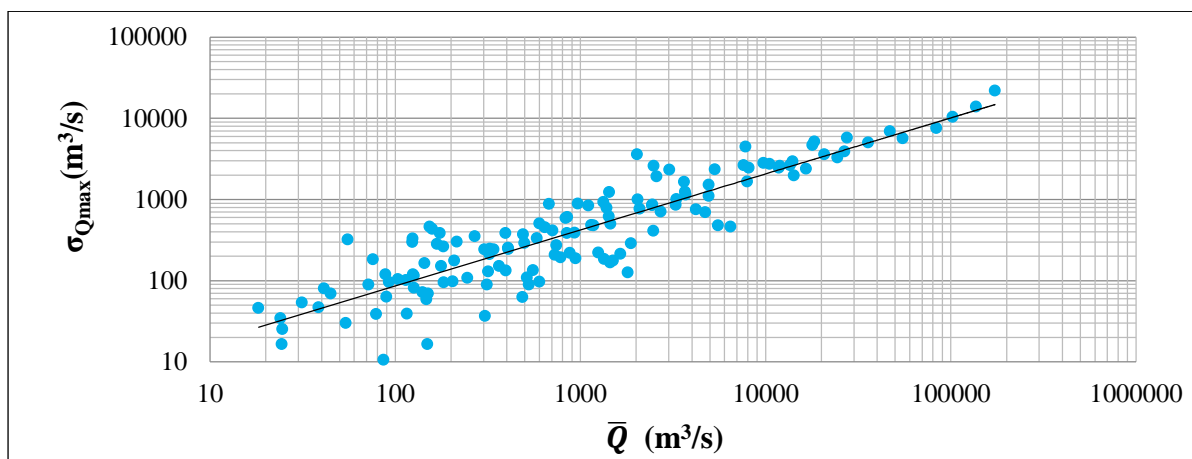


Figure 26. Closure of the water balance equation for the entire set of river gauging stations, using diverse combination of Precipitation and Evapotranspiration data sets.



**Figure 27.** Scaling between the mean of annual floods and the long-term mean river flow at all river gauging stations.



**Figure 28.** Scaling between the standard deviation of annual floods and the long-term mean river flow at all river gauging stations.

**Table 2.** Amazon Basin and Sub-Basins scaling coefficients between the mean and standard deviation of the annual floods and the long term mean river flows.

Basin	$\theta_1$	$\alpha_1$	$R^2$	$\theta_2$	$\alpha_2$	$R^2$
<b>Amazonas</b>	<b>0.85</b>	<b>7.76</b>	<b>0.96</b>	<b>0.69</b>	<b>3.62</b>	<b>0.81</b>
Branco	0.68	28.92	0.90	0.59	11.75	0.76
Jiparana	0.93	4.88	0.99	0.77	2.08	0.85
Jurua	0.71	22.86	0.97	0.37	23.17	0.51
Madeira	0.92	4.83	0.98	0.81	1.52	0.91
Mamore	0.94	3.34	0.98	0.91	0.60	0.86
Negro	0.80	11.04	0.92	0.61	6.60	0.69
Purus	0.66	35.56	0.90	0.28	57.27	0.32
Solimoes	0.75	17.33	0.96	0.58	6.84	0.75
Tapajos	0.93	3.65	0.97	0.83	1.18	0.87
Xingu	1.03	2.28	0.99	0.98	0.69	0.97

### 5.4. Maximum River Flows - Present (1970-2008) vs. Future (2009- 2050)

Estimated values of the parameters of equations (2) and (3), namely the pre-factors and scaling exponent were estimated using INLAND model outputs for the present (1970-2008) and future (2009-2050, scenario A), as shown in figures 27 and 28.

Using these relationships and the statistical scaling theory ((1 to (3), extreme river flows for different return periods, both historical and future ones, were estimated and compared to evaluate the effects of the studied land-use and climate change scenarios over the extreme flows in the Amazon River Basin. Some of the results are shown in figures 29 and 30 and table 3.

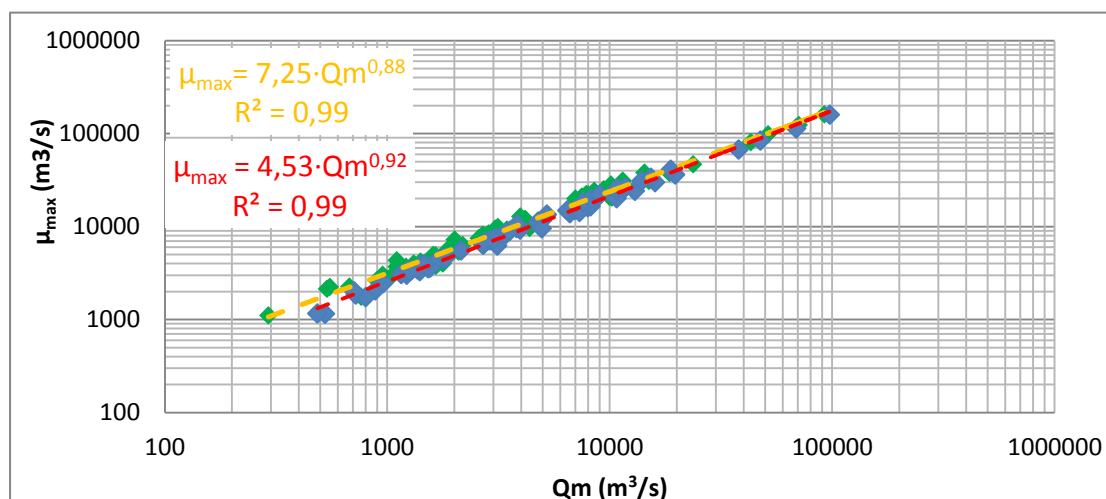


**Figure 29.** Power law relating mean flow with the mean of annual maximum flows. (INLAND model results for Present and Future Scenario A).

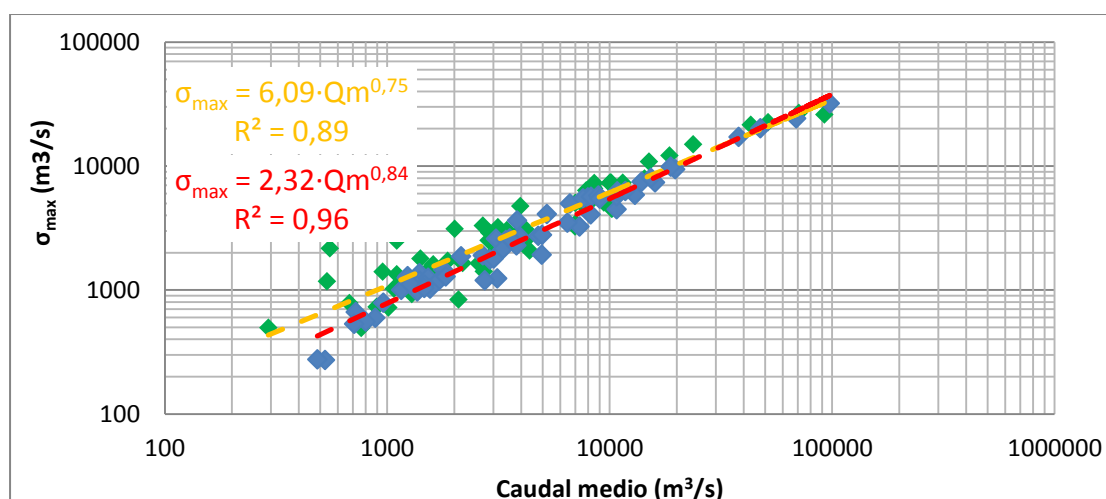


**Figure 30.** Power law relating mean flow with the standard deviation of annual maximum flows. (INLAND model results for Present and Future Scenario A).

**Table 3.** Comparison between maximum river flows of different return periods for the present (1970-2008, INLAND) and the future (2009-2050, INLAND scenario A) at three Amazon River Gauging stations.

Tr (years)	17050001 Obidos (Amazonas)			12840000 Gaviao (Jurua)			15700000 Manicore (Madeira)		
	Present (m <sup>3</sup> /s)	Future (m <sup>3</sup> /s)	Change (%)	Present (m <sup>3</sup> /s)	Future (m <sup>3</sup> /s)	Change (%)	Present (m <sup>3</sup> /s)	Future (m <sup>3</sup> /s)	Change (%)
2	160,38	159,60	-0.49	9,27	9,22	-0.49	31,04	33,36	+7.49
10	193,72	200,58	+3.54	13,16	12,65	-3.87	40,40	43,60	+7.93
25	205,93	215,58	+4.69	14,59	13,91	-4.66	43,83	47,35	+8.04
50	213,81	225,27	+5.36	15,51	14,72	-5.09	46,04	49,77	+8.11
100	220,90	233,99	+5.92	16,34	15,45	-5.44	48,03	51,95	+8.16

## 5.5. Conclusions

- Marginally, ORCHIDEE E combinations exhibit the lowest errors in the closure of the long-term water balance equation.
- Combining the long-term water balance equation and statistical scaling allow estimating extreme river flows (floods of different return periods) at any site along the entire drainage network of the Amazon River basin.
- Results for future scenarios (INLAND A & B) suggest that average and extreme flows regimes are likely to be affected by climate change. Scaling characteristics and magnitude of floods change differently, depending on the respective sub-basin.
- On-going research is aimed at involving diverse AMAZALERT climate and land-use change model and scenarios.

## 6. References

- ANA - AGÊNCIA NACIONAL DE ÁGUAS (2013), **HIDROWEB**. Base de dados hidrológicos, <http://hidroweb.ana.gov.br>
- Aguiar, A. P. D., Ometto, J. P., Nobre, C., Lapola, D. M., Almeida, C., Vieira, I. C., Soares, J. V., Alvala, R., Saatchi, S., Valeriano, D. & Castilla-Rubio, J. C. (2012) Modeling the spatial and temporal heterogeneity of deforestation-driven carbon emissions: the INPE-EM framework applied to the Brazilian Amazon *Global Change Biology* 18(11), 3346-3366.
- BÁRDOSSY, A.; PEGRAM, G. (2011), Downscaling precipitation using regional climate models and circulation patterns toward hydrology. **Water Resources Research**, v.47, doi:10.1029/2010WR009689
- BEVEN, K.J.; KIRKBY, M.J. (1979), A physically based variable contributing area model of basin hydrology, **Hydrological Sciences Bulletin**, 24, 43-69.
- Biemans, H., I. Haddeland, P. Kabat, F. Ludwig, R. W. A. Hutjes, J. Heinke, W. von Bloh, and D. Gerten (2011), Impact of reservoirs on river discharge and irrigation water supply during the 20th century, *Water Resources Research*, 47.
- COLLINS, M.; TETT, S.F.B.; COOPER, C. (2001), The internal climate variability of a HadCM3, a version of the Hadley centre coupled model without flux adjustments. **Clim Dyn**, 17:61–81, doi:10.1007/s003820000094
- Collins, W. J. *et al.* (2008), Evaluation of the HadGEM2 model., **HCTN 74**, Met Office Hadley Centre Technical Note, Met Office, UK.
- Collischonn, B ; Collischonn, W ; Tucci, C . Daily hydrological modeling in the Amazon basin using TRMM rainfall estimates. *Journal of Hydrology (Amsterdam)*, p. 207, 2008.
- CHOU, SC.; MARENGO, J.; LYRA, AA.; SUEIRO, G.; PESQUERO, JF.; ALVES, LM; KAY, G.; BETTS, R.; CHAGAS, DJ.; GOMES, JL.; BUSTAMANTE, JF. (2011), Downscaling of South America present climate driven by 4-member HadCM3 runs. *Climate Dynamics*, 38:635–653. DOI 10.1007/s00382-011-1002-
- Chow, V.T. (1951). A general formula for hydrologic frequency analysis. *Transactions, American Geophysical Union*, 32, pp. 231-237.
- DUFRESNE, J.L. *et al.* (2013), Climate change projections using the IPSL-CM5 Earth System Model: from CMIP3 to CMIP5. **Clim Dyn**, 40:2123–2165.
- EMBRAPA - EMPRESA BRASILEIRA DE PESQUISA AGROPECUÁRIA (1980), **Estudo expedito de solos do Território Federal de Rondônia para fins de classificação, correlação e legenda preliminar**. Rio de Janeiro: Serviço Nacional de Levantamento e Conservação de Solos - EMBRAPA, 145pp. (EMBRAPA-SNLCS. Boletim Técnico n. 73).
- EPE - EMPRESA DE PESQUISA ENERGÉTICA - EPE (2013), **Balço Energético Nacional 2013 – Ano base 2012: Relatório Síntese**. Rio de Janeiro: EPE.
- Espinoza Villar, J.C. . Spatio-temporal rainfall variability in the Amazon basin countries (Brazil, Peru, Bolivia, Colombia, and Ecuador). *International Journal of Climatology*, v. 29, p. 1574-1594, 2009. DOI: 10.1002/joc.1791
- GASH, J.H.C.; LLOYD, C.R.; LACHAUD, G. (1995), Estimating sparse forest rainfall interception with an analytical model. **Journal of Hydrology**, 170, 79-86.

- Guimberteau, M., Drapeau, G., Ronchail, J., Sultan, B., Polcher, J., Martinez, J. M., Prigent, C. Guyot, J-L, Cochonneau, G., Espinoza, J.C., Filizola, N., Fraizy, P., Lavado, W., Oliveira, E., Pombosa, R., Noriega, L., Vauchel, P. (2012). Discharge simulation in the sub-basins of the Amazon using ORCHIDEE forced by new datasets. *Hydrology and Earth System Sciences*, 16, 911-93.
- GORDON, C. *et al.* (2000), The simulation of SST, sea ice extents and ocean heat transport in a version of the Hadley centre coupled model without flux adjustments. **Clim Dyn**, 16:147–168.
- HAY, L.E. *et al.* (2000), A comparison of delta change and downscaling GCM scenarios for three mountainous basins in the United States. **J. Am. Water Res. Ass.**, 36, 387-398.
- IBGE - INSTITUTO BRASILEIRO DE GEOGRAFIA ESTATÍSTICA (1992), **Manual técnico de vegetação brasileira**, Rio de Janeiro, 92pp.
- JARVIS, N.J. (1989), A simple empirical model of root water uptake. *Journal of Hydrology*, 107, 57-72.
- KRAUSE, P.; BOYLE, D.P.; BÄSE, F. (2005), Comparison of different efficiency criteria for hydrological model assessment. **Advances in Geosciences**, 5, 89–97.
- LEITE, C. C.; COSTA, M. H.; SOARES-FILHO, B. S.; HISSA, L. B. V. (2012). Historical land use change and associated carbon emissions in Brazil from 1940 to 1995. **Global Biogeochemical Cycles**, v. 26, p. 2011-2029
- LEY, R.; CASPER, M.C.; HELLEBRAND, H.; MERZ, R. (2011), Catchment classification by runoff behaviour with self-organizing maps (SOM). **Hydrol. Earth Syst. Sci.**, 15, 2947–2962, doi:10.5194/hess-15-2947-2011
- MARENGO, J.; CHOU, S. C.; KAY, G.; ALVES, LM.; PESQUERO, JF.; SOARES, WR.; SANTOS, DC.; LYRA, A.A.; SUEIRO, G.; BETTS, R.; CHAGAS, DJ.; GOMES, JL.; BUSTAMANTE, JF.; TAVARES, P. (2011a), Development of regional future climate change scenarios in South America using the Eta CPTEC/HadCM3 climate change projections: climatology and regional analyses for the Amazon, São Francisco and the Paraná River basins. **Climate Dynamics**, 38:1829–1848. DOI 10.1007/s00382-011-1155-5
- Marengo, J.A., Tomasella, J., Alves, L.M., Soares, W. R., Rodriguez, D.A. (2011). The drought of 2010 in the context of historical droughts in the Amazon region. *Geophysical Research Letters*, 38, L12703, doi:10.1029/2011GL047436
- MMA - MINISTÉRIO DO MEIO AMBIENTE (2006), **Caderno da Região Hidrográfica Amazônica** / Ministério do Meio Ambiente, Secretaria de Recursos Hídricos. – Brasília: MMA.
- Mohor, G.S; Rodriguez, D.A.; Tomasella, J. Siqueira Júnior, J.L. Exploratory analyses for the assessment of climate change impacts on the energy production in an amazon run-of-river hydropower plant - *Journal of Hydrology: Regional Studies* - Submitted 2014
- Molinier M, Guyot JL, Oliveira E, Guimarães V. 1996. Les regimes hydrologiques de l'Amazonie et de ses affluents. In *L'hydrologie tropicale: géoscience et outil pour le développement*. IAHS Publishers: Mai, Paris; 209–222.
- MORIASI, D.N., ARNOLD, J.G., VAN LIEW, M.W., BINGNER, R.L., HARMEL, R.D. AND VEITH, T.L. (2007), Model evaluation guidelines for systematic quantification of accuracy in watershed simulations. **Transactions of the ASABE**, 50(3), 885-900.
- NAKICENOVIC, N.; ALCAMO, J.; DAVIS, G.; DE VRIES, B.; FENHANN, J.; GAFFIN, S.; GREGORY, K.; GRUBLER, A.; JUNG, T.Y.; KRAM, T.; LA ROVERE, E.L.; MICHAELIS, L.; MORI, S.; MORITA, T.; PEPPER, W.; PITCHER, H.; PRICE, L.; RIAHI, K.; ROEHL, A.; ROGNER, H.-H.; SANKOVSKI, A.; SCHLESINGER, M.; SHUKLA, P.; SMITH, S.; SWART, R.; VAN ROOIJEN, S.; VICTOR, N.; DADI, Z.

- (2000), **IPCC Special Report on Emissions Scenarios**. Cambridge University Press, Cambridge, United Kingdom and New York, NY, USA. pp. 599.
- Poveda, G., and co-authors (2007). Linking long-term water balances and statistical scaling to estimate river flows along the drainage network of Colombia. *Journal of Hydrologic Engineering*, 12(1), 4-13.
- Rodriguez, D. A.; Impactos dos padrões espaciais da vegetação nas variáveis atmosférica e terrestre do ciclo hidrológico, em bacia de floresta amazônica. 2011. 208 f. Tese (Doutorado em Meteorologia), Instituto Nacional de Pesquisas Espaciais, São José dos Campos, 2011. available on: <http://mtc-m18.sid.inpe.br/col/sid.inpe.br/mtc-m18/2011/02.23.18.55/doc/publicacao.pdf>
- Rodriguez, D.A., Tomasella, J., Linhares, C. (2010). Is the forest conversion to pasture affecting the hydrological response of Amazonian catchments? Signals in the Ji-Paraná Basin. *Hydrological Process*. **24**, 1254–1269 .
- Rost, S., D. Gerten, A. Bondeau, W. Lucht, J. Rohwer, and S. Schaphoff (2008), Agricultural green and blue water consumption and its influence on the global water system, *Water Resour. Res.*, **44**, W09405, doi:10.1029/2007WR006331.
- Rotstayn, L.D.; Collier, M.A.; DIX, M.R.; FENG, Y.; GORDON, H.B.; O'FARRELL, S.P.; SMITH, I.N.; SYKTUS, J.I. (2010), Improved Simulation of Australian Climate and ENSO-related rainfall variability in a global climate model with interactive aerosol treatment. *Int. J. Climatol*. 30: 1067-1088, doi:10.1002/joc.1952
- SELLERS, P. J; MINTZ, Y.; SUD, Y. C.; *et al.* (1986), A Simple Biosphere Model (SiB) for use within general circulation models. *Journal of the Atmospheric Sciences*, 43, 6, 505-531.
- SESTINI, M. F.; ALVALÁ, R. C. S.; MELLO, E. M. K. *et al.* (2002), **Elaboração de mapas de vegetação para utilização em modelos meteorológicos e hidrológicos**. São José dos Campos. INPE-8972-RPQ/730.
- Sheffield, J., G. Goteti, and E. F. Wood, 2006: Development of a 50-yr high-resolution global dataset of meteorological forcings for land surface modeling, *J. Climate*, **19** (13), 3088-3111
- Siqueira Júnior, J.L.; Tomasella, J. Rodriguez, D.A. Impacts of future climatic and land cover changes on the hydrological regime of the Madeira River basin - Climatic Change - Submitted - 2014
- Soares-Filho, B.S., D.C. Nepstad, et al., 2006. Modelling conservation in the Amazon basin. *Nature*, 440, 520-523.
- TAYLOR, K.E.; STOUFFER, R.J. AND MEEHL, G.A. (2012), An overview of CMIP5 and the experimental design. *Bulletin of the American Meteorological Society* 93: 485-498.
- Tomasella, J., Rodriguez, D.A. A numerical approach for modelling sub-grid variability in tropical catchment . *Hydrological Processes* - 2014 - Under Review.
- THOMSON, A.M. *et al.* (2011), RCP4.5: A Pathway for Stabilization of Radiative Forcing by 2100. *Climatic Change*. 109:1-2, 77-94. doi:10.1007/s10584-011-0151-4
- VOGEL, R.M.; FENESSEY, N.M. (1994), Flow-Duration Curves I: New Interpretation and Confidence Intervals. *J. Water Resour. Plann. Manage.*, 120:485-504.
- VOGEL, R.M.; FENESSEY, N.M. (1995), Flow-Duration Curves II: Review of Applications in Water Resources Planning. *Water Resources Bulletin*, 31, 6.

WATANABE, M. *et al.* (2010), Improved Climate Simulation by MIROC5: Mean States, Variability, and Climate Sensitivity. **Journal of Climate**, 23, 6312–6335.

doi:10.1175/2010JCLI3679.1

Yilmaz, K. K., H. V. Gupta, and T. Wagener (2008), A process-based diagnostic approach to model evaluation: Application to the NWS distributed hydrologic model, *Water Resources Res.*, 44, W09417, DOI:10.1029/2007WR006716

ZHAO, R.J. (1992), The Xinanjiang model applied in China. **Journal of Hydrology**, 135, 371–381.